

**People's Democratic Republic of Algeria Ministry of Higher Education
and Scientific Research**

University M'Hamed BOUGARA – Boumerdes



**Institute of Electrical and Electronic Engineering Department of
Power and Control**

Final Year Project Report Presented in Partial Fulfilment of the Require-
ments for the Degree of

MASTER in Power Engineering

Option: Power Engineering

Title: Variable Frequency Drive (VFD)

Presented by:

- GHAZI Abdenour Adel.
- HAMAILI Lyazid.

Supervisor:

Dr.METIDJI Brahim.

Cosupervisor:

Dr.ABDELKARIM Ammar.

Registration Number:/2019

Abstract

A variable frequency drive (VFD) is a type of motor controller that drives an electric motor by varying the frequency and voltage supplied to the electric motor. Other names of a VFD are variable speed drive, adjustable speed drive, adjustable frequency drive, AC drive, Microdrive, and inverter. One of the most recent variable frequency drive control methods is the Vector control also known as Field oriented control, which can be implemented through direct or indirect approaches. Indirect rotor field-oriented control (IRFOC) is a very popular technique in industries due to its simple designing and structure, in comparison to the direct method since it requires flux and torque estimators. In this proposed project IRFOC is simulated using MATLAB/Simulink and an implementation is carried out.

Dedication

*I dedicate this work to my dear parents, my brothers and sisters and
to all my family and friends.*

All my teachers that supported me during my studies.

Lyazid,

*I would like to dedicate this work to my lovely supportive family and
friends.*

*To my parents, who have been a source of encouragement and
inspiration to me throughout my life.*

Abdenour Adel,

Acknowledgements

We gratefully thank Mr.Metidji Brahim the teacher/Supervisor for his guidance and help, Mr.Ammar Abdelkarim the Cosupervisor.We would like to thank our dear camarads for their moral support through this long project. we are also thankful to the institute teachers for their continuous support.

Table of Contents

Abstract	i
<i>Dedication</i>	ii
<i>Acknowledgements</i>	iii
Table of Contents.....	iv
List of Tables.....	vi
List of Figures	vii
List of Abbreviations	ix
General Introduction	1
Thesis Organization	2

Chapter 1: Three phase Induction motor

1.1 Introduction	3
1.2 Construction of induction motor.....	3
1.2.1 Stator construction.....	4
1.2.2 Rotor construction.....	4
1.3 Principle of operation.....	5
1.3.1 Slip	6
1.3.2 Equivalent circuit.....	6
1.3.3 Torque slip relationship	7
1.4 Classification of induction motor	8
1.5 Starting of 3-phase induction motors	8
1.5.1 Resistance starting Rotor	9
1.5.2 Direct-on-line starting	9
1.5.3 Star-delta starting	9
1.5.4 Auto-transformer starting.....	10
1.5.5 Variable frequency drives starting	11
1.6 Dynamic model of induction motor in space vector form	11
1.6.1 The (a,b,c) → (α, β) Projection (Clarke Transformation)	12
1.6.2 The (α, β) → (d,q) Projection (Park Transformation).....	12
1.7 Conclusion.....	13

Chapter 02: Control Techniques of Induction Motor

2.1 Introduction	14
2.2 Scalar control.....	14
2.2.1 Constant Volts/Hz control	14
2.2.2 Constant Slip-Speed control	14
2.2.3 Constant air gap flux control.....	15
2.3 Vector control	15
2.3.1 Direct torque control (DTC).....	15
2.3.2 Rotor field-oriented control (FOC) technique	16
2.4 Three phase inverter	16
2.5 Conclusion	19
Chapter 03: Indirect Rotor Field oriented control of Induction Motor	
3.1 Introduction	20
3.2 Field Oriented Control.....	20
3.3 Rotor-field-oriented control	21
3.4 DQ-TO-ABC Transformation.....	22
3.5 Field weakening control.....	23
3.6 Hysteresis band Pulse Width Modulation current control ‘PWM HBPWM’	23
3.7 Conclusion.....	25
Chapter 04: Simulation results	
4.1 Introduction	26
4.2 Calculations for parameter determination	26
4.2.1 DC test	26
4.2.2 No load test.....	26
4.2.3 Blocked rotor test	27
4.2.4 Mechanical parameters determination	28
4.3 Proposed methodology and its design.....	30
4.3.1 Calculation of rated torque	30
4.3.2 Calculation of rated flux.....	30
4.3.3 Speed controller	30
4.3.4 Selection of dc voltage	31
4.4 Development of simulink model.....	31
4.4.1 Speed regulator block.....	31
4.4.2 IRFOC block.....	31

4.4.3 Current regulation	32
4.4.4 Simulink model of Indirect Rotor Field Oriented Induction Motor	32
4.5 Setting of the simulation parameters	33
4.6 Simulation results and discussion	35
4.7 Conclusion	38
Chapter 05: Implementation and discussion	
5.1 Introduction	39
5.2 Operation description	39
5.3 DSP Description.....	40
5.4 Current sensor circuit	40
5.5 Speed Measurement Circuit	41
5.6 Software implementation.....	41
5.6.1 The ADC assignment.....	41
5.6.2 Calibration of the ADC of DSP TMS320f28027f.....	42
5.6.3 G.P.I.O configuration	42
5.7 Hardware implementation.....	42
5.8 Implementation results	43
5.8.1 Open loop operation	43
5.8.2 Closedloop operation.....	45
5.9 Conclusion	47
General conclusion	48
References	49
Appendix A	51

List of Tables

Table2.1 Inverter Switching states.....	18
Table4.1 Active and reactive power computations at different voltages.....	29

List of Figures

Figure1. 1 Construction of induction motor	3
Figure1.2 Stator construction	4
Figure1.3 Squirrel cage rotor	4
Figure1.4 Wound rotor construction	5
Figure1.5 Equivalent circuit of induction motor	7
Figure1.6 Torque Speed characteristic	7
Figure1.7 Rotor resistance starting	9
Figure1. 8 Delta star starting	10
Figure1.9 Autotransformer starting	11
Figure1.10 Clarke Transformation using the complex vector 'U'	12
Figure2.1 The standard three-phase inverter	17
Figure3.1 Torque control of DC motors	20
Figure3.2 Orientation of d-axis of 'dq' rotating frame toward the Ψ_r -axis	21
Figure3.3 Block diagram of indirect rotor field oriented control scheme	22
Figure3.4 Principle of Hysteresis Band current control	23
Figure4.1 Equivalent circuit of no-load test	27
Figure4.22 Equivalent circuit of blocked rotor test	27
Figure4.3 Slow down curve	29
Figure4.4 Speed regulator block	31
Figure4.5 IRFOC block	32
Figure4.6 Simulink model of Hysteresis current controller	32
Figure4.7 Model of indirect rotor field oriented induction motor	33
Figure4.8 Transfer function relating the torque to speed	34

Figure4.9 Rotor speed vs time	35
Figure4.10 Output torque	35
Figure4.11 Stator currents	35
Figure4.12 Rotor fluxes	36
Figure4.13 Rotor speed.....	36
Figure4.14 Stator currents	37
Figure4.15 Slip speed	37
Figure5.1 Current sensor circuit.	40
Figure5.2 All of the module components	41
Figure5.3 Implementation test bench	43
Figure5.4 Openloop operation algorithm	43
Figure5.5 Current Probes.....	44
Figure5.6 Current Waveforms	44
Figure5.7 Gate signals waveform.....	45
Figure5.8 Closedloop operation algorithm.....	45
Figure5.9 Current waveform	46
Figure5.10 Speed measurement of taco generator	46

List of Abbreviations

DTC	Direct torque control
FOC	Field oriented control
VFD	Variable frequency drive
AC	Alternating current
PI	Proportional integrator
DSP	Digital signal processing
IRFOC	Indirect rotor field oriented control
IM	Induction motor
EMF	Electromotive force
NEMA	National Electrical Manufacturers Association
α-β	coordinates of Clarke transformation
d-q	coordinates of park transformation
DC	Direct current
VSI	Voltage source inverter
CSI	Current source inverter
PWM	Pulse width modulation
KVL	Kirchhoff's voltage law
KCL	Kirchhoff's current law
HBPWM	Hysteresis band pulse width modulation
ADC	Analog to digital converter
CPU	Central processing unit

General Introduction

The Induction motor is widely used in the industrial applications. This motor is also used for domestic and commercial applications. The three-phase induction motors are almost 70% of the machines used in industries [1]. It is robust, reliable and with low maintenance fees. In most concerned fields, a precise control is required, thus many control methods have been developed depending on the demand such as direct torque control (DTC), field oriented control (FOC).

Vector control, also called field-oriented control (FOC), is a variable-frequency drive (VFD) control method in which the stator currents of a three-phase AC electric motor are identified as two orthogonal components that can be visualized with a vector. One component defines the magnetic flux of the motor, the other the torque. The control system of the drive calculates the corresponding current component references from the flux and torque references given by the drive's speed control. The pulse-width modulation of the variable-frequency drive defines the transistor switching states.

FOC was originally developed for high-performance motor applications that are required to operate smoothly over the full speed range and have high dynamic performance including fast acceleration and deceleration. Furthermore, the need for a fast response in real time requires the use of a DSP microcontroller. A Digital Signal Processor, or DSP, is a specialized microprocessor that has an architecture which is optimized for the fast-operational needs of digital signal processing. A Digital Signal Processor (DSP) can process data in real time, making it ideal for applications that can't tolerate delays [2].

This is the reason why our project will further discuss the indirect rotor field oriented control technique using the DSP board.

Thesis Organization

This thesis consists of five chapters. Chapter 1 is an introduction on the three-phase induction motor. In Chapter 2 the control Techniques of the Induction Motor. Chapter 3 covers the basic principles of Indirect Rotor Field Oriented Control Induction Motor. Chapter 4 is devoted to the simulation of the different block components of the IRFOC simulation Algorithm with results discussion. Chapter 5 is on the implementation of the IRFOC on the test bench with the experimental results discussion, followed by the general conclusion.

Chapter 1: Three phase Induction motor

1.1 Introduction

An induction motor (IM) is an asynchronous AC machine where power is supplied to the rotating device by means of electromagnetic induction, Induction motors are now the preferred choice for industrial motors due to their rugged construction, absence of brushes and the ability to control the speed of the motor. However only over the past few years that the full potential of the controllability of these motors has been reached. This is due to the development of more powerful microprocessors that can compute long algorithms much faster.

1.2 Construction of induction motor

A typical motor consists of two parts namely stator and rotor like other type of motors.

1. An outside stationary stator having coils supplied with AC current to produce a rotating magnetic field.
2. An inside rotor attached to the output shaft that is given a torque by the rotating field.

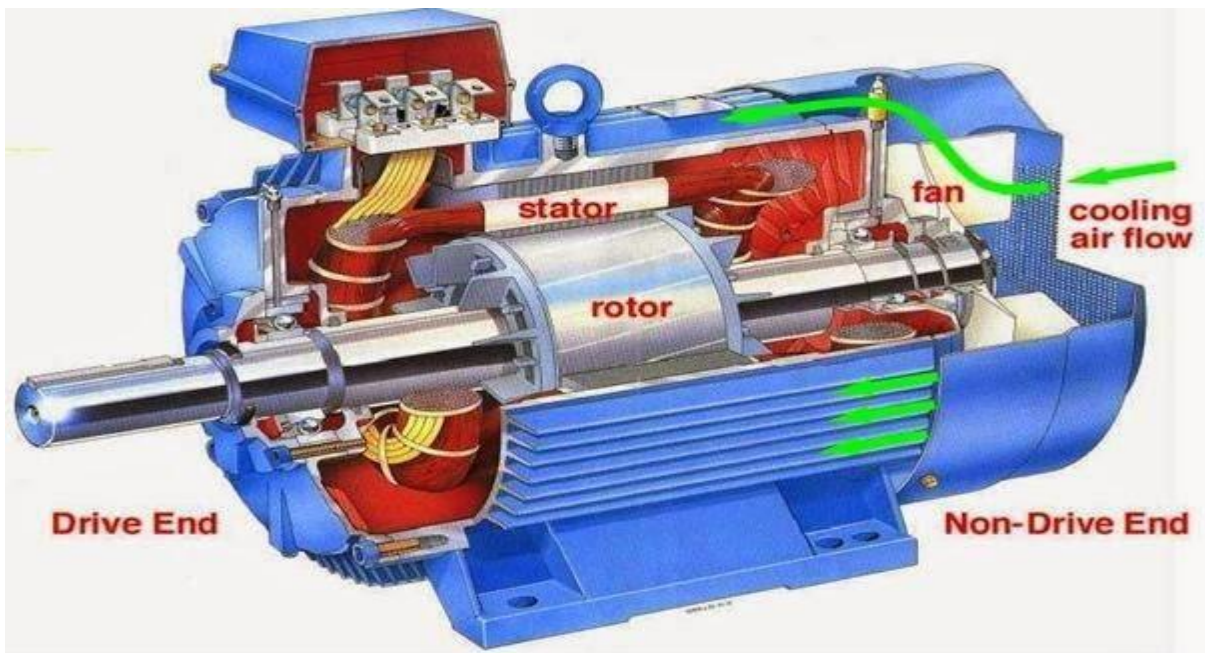


Figure1. 1 Construction of induction motor

1.2.1 Stator construction

The stator of an induction motor is laminated iron core with slots similar to a stator of a synchronous machine coils are placed in the slots to form a three- or single-phase winding [3].

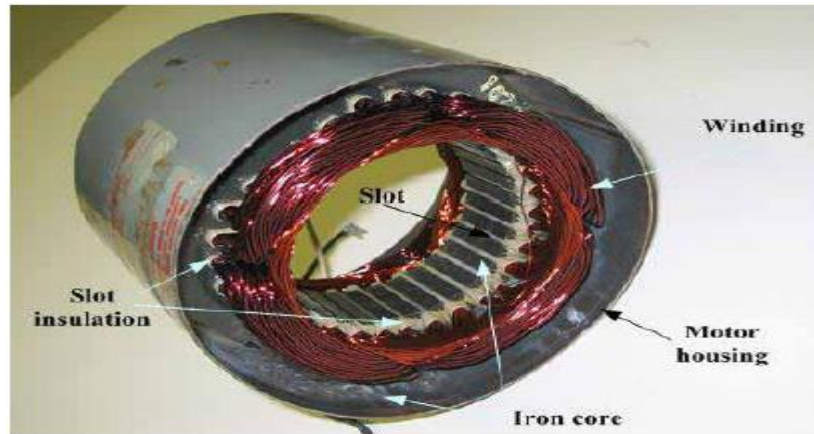


Figure1.2 Stator construction

1.2.2 Rotor construction

The rotor is made up of several thin steel laminations with evenly spaced bars, which are made up of aluminum or copper, along the periphery.

Types of rotor:

a- Squirrel cage rotor

The rotor winding consists of single copper or aluminum bars placed in the slots and short-circuited by end-rings on both sides of the rotor [3].

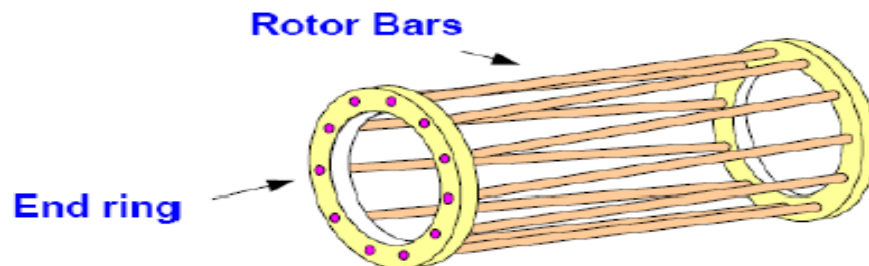


Figure1.3 Squirrel cage rotor

b- Wound rotor

In the wound rotor, an insulated 3-phase winding is placed in the rotor slots. The ends of the star-connected rotor winding are brought to three slip rings on the shaft so that a connection can be made to it for starting or speed control [3].

- 1- It is usually for large 3 phase induction motors.
- 2- Rotor has a winding the same as stator and the end of each phase is connected to a slip ring.
- 3- Compared to squirrel cage rotors, wound rotor motors are expensive and require maintenance of the slip rings and brushes, so it is not so common in industry applications.

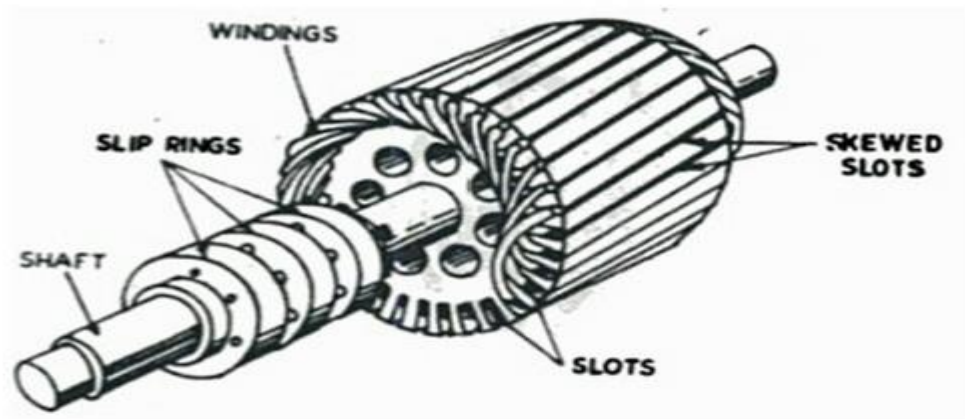


Figure1.4 Wound rotor construction

1.3 Principle of operation

- An AC current is applied in the stator armature which generates a flux in the stator magnetic circuit.
- This flux induces an emf in the conducting bars of rotor as they are “cut” by the flux while the magnet is being moved ($E = BVL$ (Faraday’s Law))
- A current flow in the rotor circuit due to the induced emf, which in term produces a force, ($F = BIL$) can be changed to the torque as the output.

In a 3-phase induction motor, the three-phase currents i_a , i_b and i_c , each of equal magnitude, but differing in phase by 120° . Each phase current produces a magnetic flux and there is physical 120° shift between each flux. Such a magnetic flux produced by balanced

three phase currents flowing in three-phase windings is called a rotating magnetic flux or rotating magnetic field (RMF). RMF rotates with a constant speed (Synchronous Speed). This flux produces magnetic field and the field revolves in the air gap between stator and rotor. So, the magnetic field induces a voltage in the short-circuited bars of the rotor. This voltage drives current through the bars. The interaction of the rotating flux and the rotor current generates a force that drives the motor and a torque is developed consequently.

However, for these currents to be induced, the speed of the physical rotor and the speed of the rotating magnetic field in the stator must be different, or else the magnetic field will not be moving relative to the rotor conductors and no currents will be induced. This difference between the speed of the rotor and speed of the rotating magnetic field in the stator is called slip. It is unitless and is the ratio between the relative speed of the magnetic field as seen by the rotor the (slip speed) to the speed of the rotating stator field. Due to this an induction motor is sometimes referred to as an asynchronous machine [3].

1.3.1 Slip

The relationship between the supply frequency, f , the number of poles, p , and the synchronous speed (speed of rotating field in rpm), W_{sy} is given by:

$$W_{sy} = \frac{120f}{P} \quad (1.1)$$

The stator magnetic field (rotating magnetic field) rotates at a speed, W_{sy} , the synchronous speed. If, W_r = speed of the rotor. The slip, s for an induction motor is defined as:

$$s = \frac{W_{sy} - W_r}{W_{sy}} \quad (1.2)$$

The mechanical speed of the rotor, in terms of slip and synchronous speed is given by

$$W_m = (1 - s)W_{sy} \quad (1.3)$$

1.3.2 Equivalent circuit

An induction motor is sometimes called a rotating transformer because the stator (stationary part) is essentially the primary side of the transformer and the rotor (rotating part) is the secondary side.

The stator current I_s , which is drawn into the stator windings from the AC stator supply voltage V_s , can then be predicted using this model.

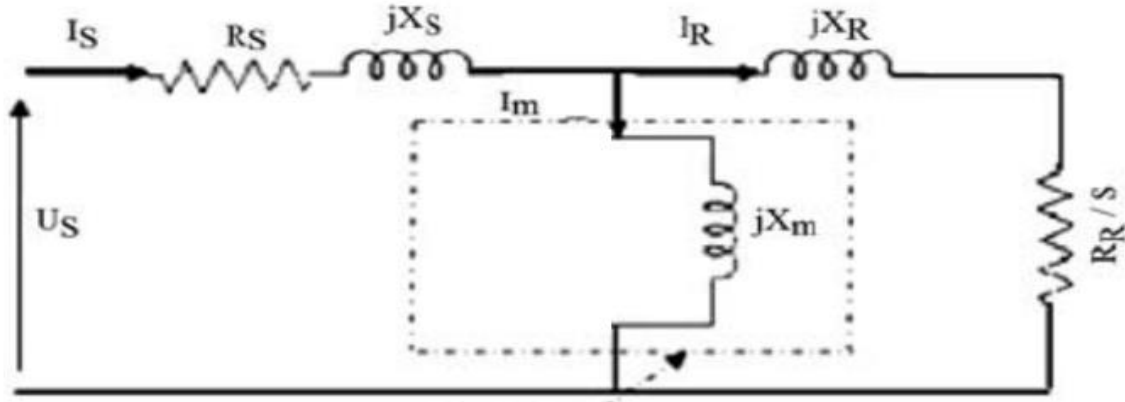


Figure1.5 Equivalent circuit of induction motor

Where: V_s = Stator supply voltage, R_s = Stator resistance, R_r = Rotor resistance,

L_s = Stator inductance, L_r = Rotor inductance, L_m = Magnetizing inductance,

I_s = Stator current, I_r = Rotor current, I_m = Magnetizing current.

1.3.3 Torque slip relationship

For small values of slip s , the torque is directly proportional to s , and for large values of slip s , the torque is inversely proportional to s [4].

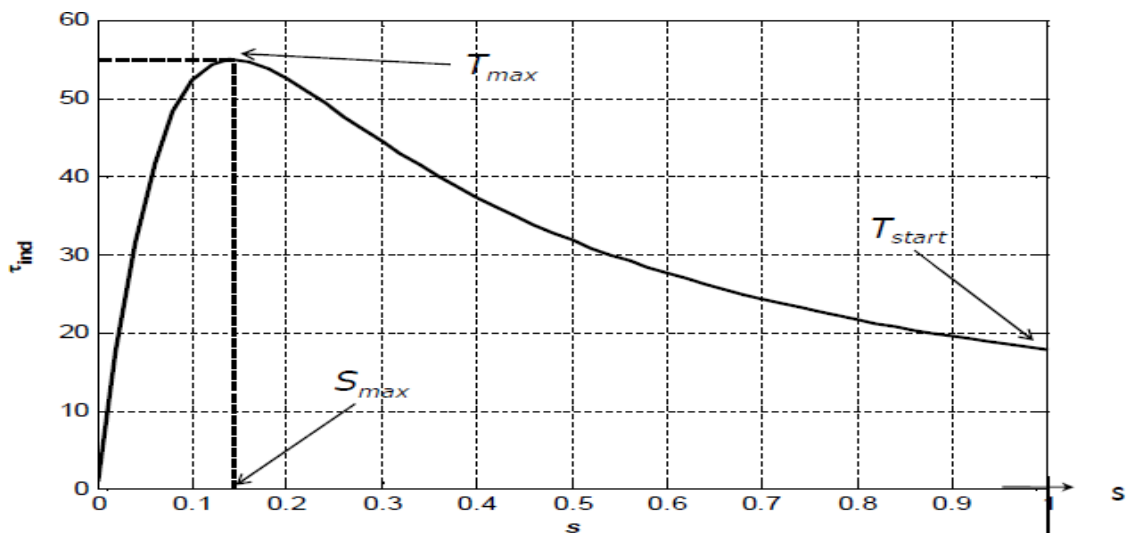


Figure1.6 Torque slip relationship

1.4 Classification of induction motor

This classification is done according to NEMA = National Electrical Manufacturers Association. The four NEMA designs have unique speed – torque –slip relationships making them suitable to different applications [3].

Class A

Max slip 5%, has high to medium starting current and normal breakdown torque, it is suited for broad variety of applications such as fans and pumps.

Class B

Max slip 5%, it has low starting current and normal breakdown torque, it is suited for broad variety of applications, normal starting applications are common in HVAC with fans, blowers.

Class C

Max slip 5%, it has low starting current and normal breakdown torque, it is suited for equipment's with high inertia.

Class D

Max slip 5-13%, Low starting current and normal breakdown torque, it is used for equipment with high inertia such as cranes, hoist etc.

1.5 Starting of 3-phase induction motors

There are two important factors to be considered in starting of induction motors:

1. The starting current drawn from the supply.
2. The starting torque.

The starting current should be kept low to avoid overheating of motor and excessive voltage drops in the supply network. The starting torque must be about 50 to 100% more than the expected load torque to ensure that the motor runs up in a reasonably short time [3].

1.5.1 Resistance starting Rotor

By adding internal resistances to the rotor circuit any starting torque up to the maximum torque can be achieved; and by gradually cutting out the resistances a high torque can be maintained throughout the starting period. The added resistances also reduces the starting current, so that a starting torque in the range of 2 to 2.5 times the full load torque can be obtained at a starting current of 1 to 1.5 times the full load current. This method is applied only for wound rotor IM.

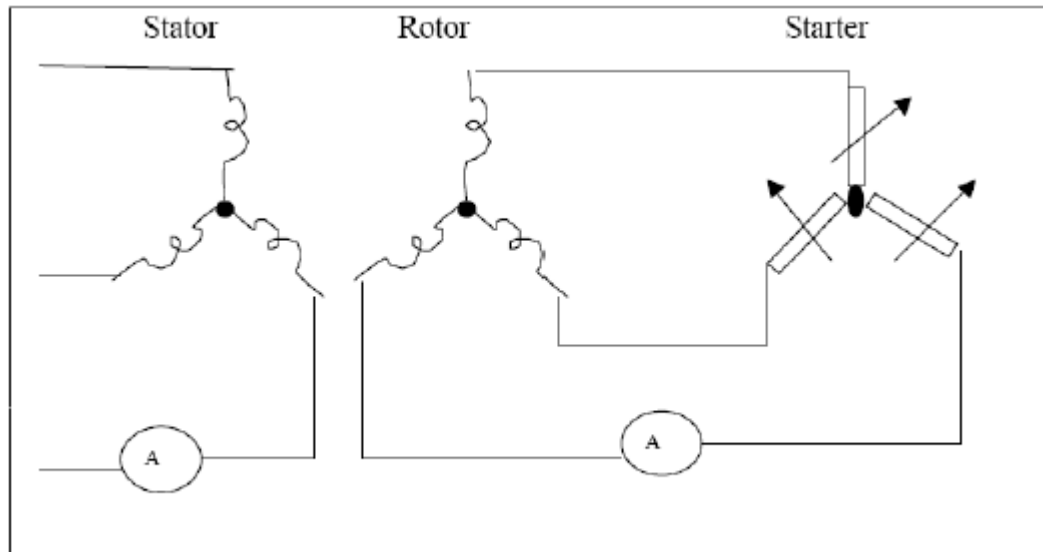


Figure1.7 Rotor resistance starting

1.5.2 Direct-on-line starting

This is the most simple and inexpensive method of starting a squirrel cage induction motor. The motor is switched on directly to full supply voltage. The initial starting current is large, normally about 5 to 7 times the rated current but the starting torque is likely to be 0.75 to 2 times the full load torque. To avoid excessive supply voltage drops because of large starting currents this method is restricted to small motors only.

1.5.3 Star-delta starting

For starting, the stator windings are connected in star and when the machine is running the switch is thrown quickly to the running position, thus connecting the motor in delta for normal operation. The phase voltages & the phase currents of the motor in star connection

are reduced to $1/\sqrt{3}$ of the direct -on -line values in delta. The line current is 1/3 of the value in delta. A disadvantage of this method is that the starting torque (which is proportional to the square of the applied voltage) is also reduced to 1/3 of its delta value [3].

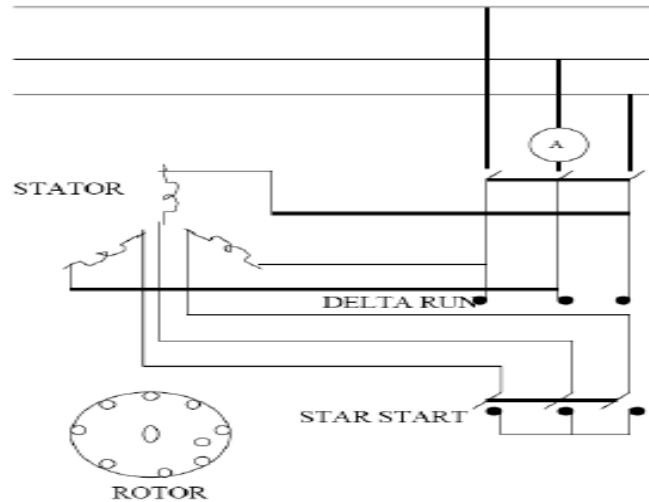


Figure1. 8 Delta star starting

1.5.4 Auto-transformer starting

This method also reduces the initial voltage applied to the motor and therefore the starting current and torque. The motor, which can be connected permanently in delta or in star, is switched first on reduced voltage from a 3-phase tapped auto -transformer and when it has accelerated sufficiently, it is switched to the running (full voltage) position. The principle is similar to star/delta starting and has similar limitations. The advantage of the method is that the current and torque can be adjusted to the required value, by taking the correct tapping on the autotransformer. This method is more expensive because of the additional autotransformer[3].

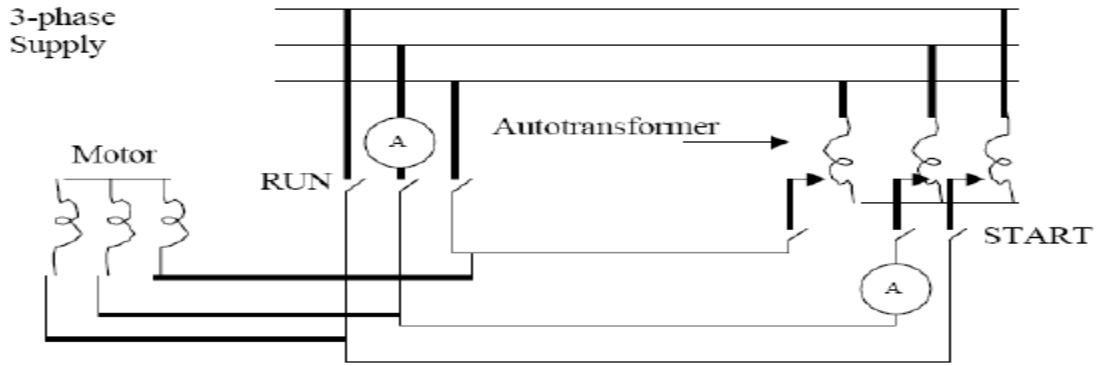


Figure1.9 Autotransformer starting

1.5.5 Variable frequency drives starting

Variable frequency drives are semiconductor devices mainly used for motor torque-speed control and protection. It can start and stop a motor smoothly. Speed torque characteristics of a motor can be controlled throughout its operation based on the application by using a VFD. Speed of the motor can be controlled from 0 to its rated speed (sometimes above the rated speed) by varying the frequency of the motor supply[5].

1.6 Dynamic model of induction motor in space vector form

Mathematical description of induction motor is based on space vector notation. When describing a three-phase induction motor by a system of nonlinear equations, the following assumptions are made [6]:

- 1- Symmetrical and balanced stator and rotor windings
- 2- Slotting effects, which are the higher order harmonics and the magneto motive force MMF, are to be disregarded.
- 3- The permeability of the iron part is infinite (no saturation which results in constant inductances).
- 4- Uniform air gap .
- 5- Skin and temperature effects are neglected (stator and rotor resistances are constant).

The space vector can be defined by considering the instantaneous values u_a , u_b , u_c . A three-phase system defined by $u_a(t)$, $u_b(t)$, $u_c(t)$ can be represented uniquely by a rotating vector. The space vector u may represent the motor variables (voltage, current and flux). The vector control principle on AC motor take the advantages of transforming the variables from

the physical three phase a - b - c system to a stationary coordinate α - β (the Clarke transformation), which outputs a two-co-ordinate time variant system then to a rotating reference frame d - q (the Park transformation), which outputs a two-co-ordinate time invariant system [7].

1.6.1 The $(a,b,c) \rightarrow (\alpha, \beta)$ Projection (Clarke Transformation)

The complex vector ‘U’, represents the three-phase sinusoidal system, is represented as:

$$U = U_\alpha + jU_\beta = \frac{2}{3}(U_a(t) + U_b(t)e^{j2\pi/3} + U_c(t)e^{-j2\pi/3}) \quad (1.4)$$

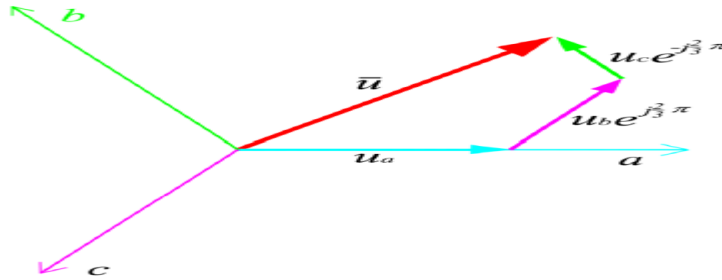


Figure1.10 Clarke Transformation using the complex vector ‘U’

$$V_{abcs} = R_s i_{abcs} + \frac{d(\Psi_{abcs})}{dt} \quad (1) \text{ stator voltage equation} \quad (1.5)$$

$$V_{abcr} = R_r i_{abcr} + \frac{d(\Psi_{abcr})}{dt} \quad (2) \text{ rotor voltage equation} \quad (1.6)$$

The voltage equations in two-phase system will be

$$V_{\alpha\beta s} = R_s i_{\alpha\beta s} + \frac{d(\Psi_{\alpha\beta s})}{dt} \quad (1.7)$$

$$V_{\alpha\beta r} = R_r i_{\alpha\beta r} + \frac{d(\Psi_{\alpha\beta r})}{dt} \quad (1.8)$$

And current equation will be

$$i_{s\alpha} = i_a \quad (1.9)$$

$$i_{s\beta} = \frac{1}{\sqrt{3}}i_a + \frac{2}{\sqrt{3}}i_b \quad (1.10)$$

1.6.2 The $(\alpha, \beta) \rightarrow (d,q)$ Projection (Park Transformation)

It consists of all the electric and magnetic quantities expressed in a reference frame which is rotating at a random speed ω_e [6].

For stator quantities:

$$V_{dqS} = V_{\alpha\beta S} e^{-j\theta_e} \quad (1.11)$$

$$i_{dqS} = i_{\alpha\beta S} e^{-j\theta_e} \quad (1.12)$$

$$\Psi_{dqS} = \Psi_{\alpha\beta S} e^{-j\theta_e} \quad (1.13)$$

For rotor quantities:

$$V_{dqr} = V_{\alpha\beta r} e^{-j(\theta_e - \theta_r)} \quad (1.14)$$

$$i_{dqr} = i_{\alpha\beta r} e^{-j(\theta_e - \theta_r)} \quad (1.15)$$

$$\Psi_{dqr} = \Psi_{\alpha\beta r} e^{-j(\theta_e - \theta_r)} \quad (1.16)$$

Resolving now the equations to real and imaginary parts, we obtain

$$V_{ds} = R_s i_{ds} + \frac{d\phi_{ds}}{dt} - \omega_e \phi_{qs} \quad (1.17)$$

$$V_{qs} = R_s i_{qs} + \frac{d\phi_{qs}}{dt} + \omega_e \phi_{ds} \quad (1.18)$$

$$V_{dr} = R_r i_{dr} + \frac{d\phi_{dr}}{dt} - (\omega_e - \omega_r) \phi_{qr} \quad (1.19)$$

$$V_{qr} = R_r i_{qr} + \frac{d\phi_{qr}}{dt} - (\omega_e - \omega_r) \phi_{dr} \quad (1.20)$$

Using the above equations, the expression of the induced torque is

$$T_e = \frac{3P}{2} \frac{L_m}{L_r} (i_{qs} \Psi_{dr} - i_{ds} \Psi_{qr}) \quad (1.21)$$

Where L_m is mutual inductance, L_r is the rotor self-inductance referred to stator, P is the number of poles.

1.7 Conclusion

This chapter has dealt with the construction of induction motor, principle of operation, classification of induction motor, starting of 3-phase induction motors and the dynamic model of induction motor in space vector form specifically the (a,b,c) \rightarrow (α , β) Projection (Clarke Transformation) and the (α , β) \rightarrow (d,q) Projection (Park Transformation).

**Chapter 02: Control
Techniques of Induction
Motor**

2.1 Introduction

An induction motor is essentially a constant-speed motor when connected to a constant-voltage and constant-frequency power supply. The operating speed is very close to the synchronous speed. If the load torque increases, the speed drops by a very small amount. It is therefore suitable for use in substantially constant-speed drive systems. Many industrial applications, however, require several speeds or a continuously adjustable range of speeds.

A general classification of the control techniques for the IM methods is made by Holtz from the point of view of the controlled signal [8].

2.2 Scalar control

These techniques are mainly implemented through direct measurement of the machine parameters.

Speed control is achieved in the inverter-driven IM by means of variable frequency. Apart from the frequency, the voltage needs to be varied to keep the air-gap flux constant and not let it to saturate.

2.2.1 Constant Volts/Hz control

When the speed of the induction motor is adjusted to values less than the nominal, the variation of the stator voltage is followed by the corresponding variation of the stator voltage frequency such that the ratio V_s/f_s to be kept constant. Keeping V_s/f_s constant the magnetic flux of the air gap is kept approximately constant.

2.2.2 Constant Slip-Speed control

The slip speed is maintained constant, therefore for different rotor speeds, the slip will be varying according to the following equation:

$$\omega_{sl} = s\omega_s = \text{constant} \quad (2.1)$$

$$\omega_s = \omega_r + \omega_{sl} \quad (2.2)$$

So, in order to maintain the slip speed constant, it is required to know the rotor speed [9].

2.2.3 Constant air gap flux control

In this technique the air gap flux level is maintained constant hence the performance of torque response time is enhanced.

The air gap flux level is given by:

$$\Phi_m = L_m i_m \quad (2.3)$$

In order to maintain the air gap flux constant, the magnetizing current must be kept constant [9].

2.3 Vector control

provides more precise torque and flux control of AC motors compared to scalar control. advanced control strategies can be implemented that use mathematical transformations in order to decouple the torque generation and the magnetization functions in an AC induction motor.

In this section 2 main methods of vector control are briefly presented.

2.3.1 Direct torque control (DTC)

In contrast with the scalar control technique, direct torque control can control independently the stator magnetic flux and the electromagnetic torque of the induction motor. The basic principle of DTC is the direct selection of a space vector and respective control signals, to control instantaneously the electromagnetic torque and stator flux magnitude. The DTC technique requires only knowledge of the stator resistance and, consequently, reduces the sensitivity associated with the parameters variation and feedback speed is not needed [10]. In the DTC as inputs are considered the desired torque and flux values.

The DTC presents the following disadvantages:

- Difficulty to control torque and flux at very low speed
- High current and torque ripple
- Variable switching frequency
- High noise level at low speed

2.3.2 Rotor field-oriented control (FOC) technique

Field-oriented control (FOC) control technique provides decoupling between the torque and magnetic flux of the motor and, consequently, fast torque response can be obtained. Unlike the scalar control the FOC technique, which uses equations and models of the induction motor dynamic state, has the ability to control the amplitude, the frequency, and the position of the space vectors of the voltages, currents, and magnetic flux. This method achieves the decoupling between the torque and magnetic flux control. FOC is divided to the following two main types :

1- Direct rotor field-oriented control (DRFOC)

When DRFOC is used the rotor flux vector (amplitude and position) is calculated directly from the measured quantities of the motor.

2- Indirect rotor field-oriented control (IRFOC)

When IRFOC is used the rotor flux (amplitude and position) is calculated indirectly from existing speed and slip estimations using the field control equations.

2.4 Three phase inverter

An inverter is a device that converts DC power, to standard AC power by switching the DC input voltage (or current) in a pre-determined sequence to generate AC voltage (or current). depending on the type of the supply source and the related topology of the power circuit. They are classified as voltage source inverters (VSIs) and current source inverters (CSIs). For the VSI the output voltage is constant, with the output current changing with the load type. But in the CSI, the current is nearly constant. The voltage changes here, as the load is changed. Single-phase VSIs cover low-range power applications and three-phase VSIs cover medium to high power applications [11]. The main purpose of these topologies is to generate controllable frequency and ac voltage magnitudes using various pulse width modulation (PWM) strategies.

Inverters can be classified according to the numbers of levels at the output:

- 1- Regular two-level Inverter: these inverters have only voltage levels at the output which are positive peak voltage and negative peak voltage.

- 2- Multilevel inverters: these inverters can have multiple voltage levels at the output this is done by increasing the number of switches, sources and capacitors.

The standard three-phase inverter is shown in the following Figure

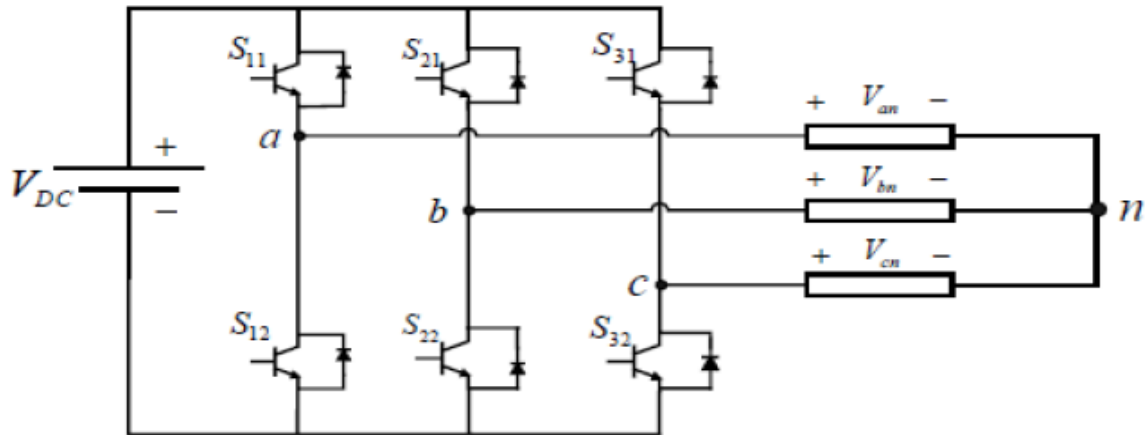


Figure2.1 The standard three-phase inverter

The output phase voltages are produced by a DC link voltage V_{dc} which is provided by a rectifier, battery pack or any other DC source.

There are two possible switching modes which are:

- 1- 180° conduction mode: In this mode of conduction, every device is in conduction state for 180° where they are switched ON at 60° intervals. The terminals A, B and C are the output terminals of the bridge that are connected to the three-phase delta or star connection of the load.
- 2- 120° conduction mode: In this mode of conduction, each electronic device is in a conduction state for 120°.

The inverter has eight switch states given in **Table 2.1**. As explained earlier in order that the circuit satisfies the KVL and the KCL, both of the switches in the same leg cannot be turned ON at the same time, as it would short the input voltage violating the KVL. Thus, the nature of the two switches in the same leg is complementary.

Table 2.1 Inverter Switching states

S_{11}	S_{21}	S_{31}	V_{ab}	V_{bc}	V_{ca}
0	0	0	0	0	0
0	0	1	0	$-V_{DC}$	V_{DC}
0	1	0	$-V_{DC}$	V_{DC}	0
0	1	1	$-V_{DC}$	0	$-V_{DC}$
1	0	0	V_{DC}	0	$-V_{DC}$
1	0	1	V_{DC}	$-V_{DC}$	0
1	1	0	0	V_{DC}	$-V_{DC}$
1	1	1	0	0	0

Of the eight switching states as shown in **Table 2.1** two of them produce zero ac line voltage at the output. In this case, the ac line currents freewheel through either the upper or lower components. The remaining states produce no zero ac output line voltages. In order to generate a given voltage waveform, the inverter switches from one state to another. Thus, the resulting ac output line voltages consist of discrete values of voltages, which are $-V_{DC}$, 0, and V_{DC} .

As far as the user is concerned, it does not really matter what type of switching device is used inside the inverter, but it is probably helpful to mention the four most important families of devices in current use:

1- Bipolar junction transistor

The advantage of the bipolar transistor is that when it is turned on by current switching signal the power dissipation is small in comparison with the load power i.e. the device is an efficient power switch, but it has a small range of rated current and voltage.

2- MOSFET

The principal advantage of the MOSFET is that it is a voltage-controlled device which requires negligible power to hold it in the on state and it has a very high switching frequency up to 1MHz. MOSFETs are used in low and medium power inverters up to a few kilowatts, with voltages generally not exceeding 700 V.

3- GTO

The GTO is turned on by a pulse of current in the gate-cathode circuit and can be turned off by a negative gate-cathode current. The GTO has considerably higher voltage and current ratings (up to 3 kV and 2 kA) and is therefore used in high-power inverters.

4- IGBT

The IGBT is a hybrid device which combines the best features of the MOSFET and the BJT, so it is turned on by a voltage switching signal and has low power dissipation. They are particularly well suited to the medium power, medium voltage range (up to several hundred kilowatts) [12].

2.5 Conclusion

This chapter dealt with Scalar control techniques such as constant Volts/Hz, constant slip-speed, constant air gap flux, then dove in the vector control techniques such as direct torque control (DTC), rotor field-oriented control (RFOC) technique and three phase inverter with its switch states and different possible switches like bipolar junction transistor, MOSFET, GTO, IGBT

Chapter 03: Indirect Rotor Field oriented control of Induction Motor

3.1 Introduction

The control methods for induction motors can be divided into two sections: scalar and vector control. The main goal of a chosen control method is to provide the best possible parameters of drive. Additionally, a very important requirement regarding the chosen control method is simplicity (simple algorithm, simple tuning and operation with small controller dimension leads to low price of final product). Indirect Field Oriented Control (IFOC) is a very popular technique in industries due to its simple designing and structure.

3.2 Field Oriented Control

Field Oriented Control can be implemented in three field or flux orientations as there are three flux linkages available in an Induction motor. They are- stator, air gap & rotor flux linkage. Rotor Flux Orientation is a technique that provides a method of decoupling the stator currents of squirrel-cage induction motor into two components in the synchronously rotating reference frame (d-q frame): one is the magnetizing current i_{ds}^* , which is to excite the motor flux and the other torque current i_{qs}^* , which is to generate the electromagnetic torque respectively. Therefore, it provides independent control of torque and flux.

Basically, there are two methods of Field Oriented control based on the way of determining the rotor angle - direct method by which rotor angle is found by measurement of the oriented flux components and indirect method in which rotor angle is obtained through computations and machine parameters [13]. Rotor field orientation (RFO) is the original and usual choice for the indirect field-oriented control. Hence the name Indirect Rotor Field orientation (IRFOC).

The developed torque T_e in a dc motor is expressed in terms of armature current and field current as shown in the figure below:

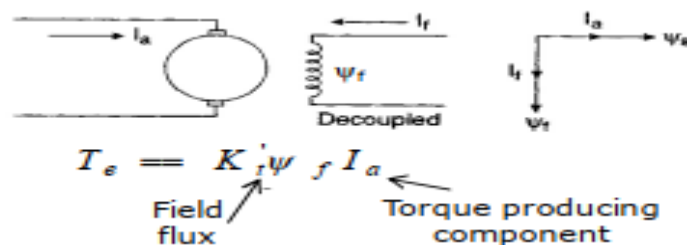


Figure3.1 Torque control of DC motors

$$T_e = K_t(\Psi_f * I_a) \quad (3.1)$$

The torque T_e developed by the induction motor is given by:

$$T_e = \frac{3}{2} \frac{P}{2} \frac{L_m}{L_r} (i_{qs} \Psi_{dr} - i_{ds} \Psi_{qr}) \quad (3.2)$$

To make the torque equation look like that of the DC motor, the second term must be null (0). This can be implemented by aligning the d-axis of the rotating reference frame (dq) with the rotor flux axis (Ψ_r) axis (or the stator flux axis(Ψ_s)). The flux to which the d-axis is oriented, determines the type of the controller whether it is rotor-field-oriented controller 'RFOC' or stator-field oriented controller 'SFOC'.

3.3 Rotor-field-oriented control

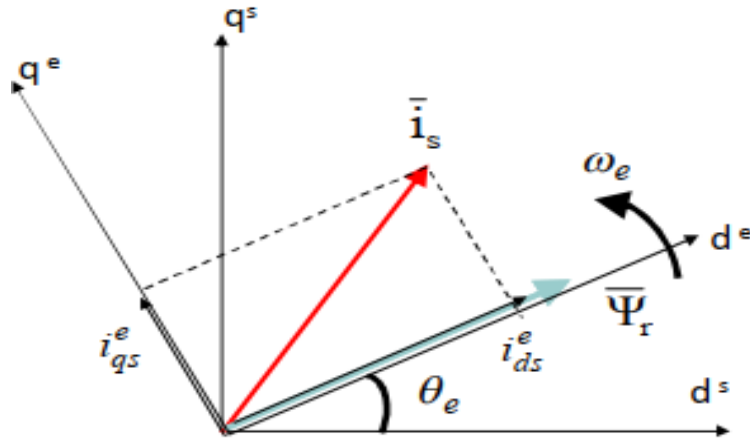


Figure3.2 Orientation of d-axis of 'dq' rotating frame toward the Ψ_r -axis

Orientation of d-axis of 'dq' rotating frame toward the Ψ_r -axis amounts to:

$\Psi_r = L_m i_{ds}$ And $\Psi_{qr} = 0$, therefore:

$$T_e = \frac{3}{2} \frac{P}{2} \frac{L_m}{L_r} i_{qs} \Psi_{dr} \quad (3.3)$$

➤ i_{qs} = torque producing current

➤ i_{ds} = field producing current

Resulting in a decoupled control, similar to a DC motor control.

The following equations will be used:

$$i_{qs}^* = \frac{2}{3} \frac{P}{2} \frac{L_r}{L_m} \frac{T_e^*}{|\Psi_r|_{ref}} \quad (3.4)$$

where L_r is the rotor inductance, L_m is the mutual inductance.

The flux producing component of stator current i_{ds}^* is:

$$i_{ds}^* = \frac{|\Psi_r|^*}{L_m} \quad (3.5)$$

The rotor flux position θ required for coordinates transformation is

$$\theta = \int (W_e + W_{sl}) dt \quad (3.6)$$

The slip frequency W_{sl} is:

$$W_{sl} = \frac{L_m}{|\Psi_r|_{ref}} \frac{R_r}{L_r} i_{qs} \quad (3.7)$$

The block diagram of the laws are as follows:

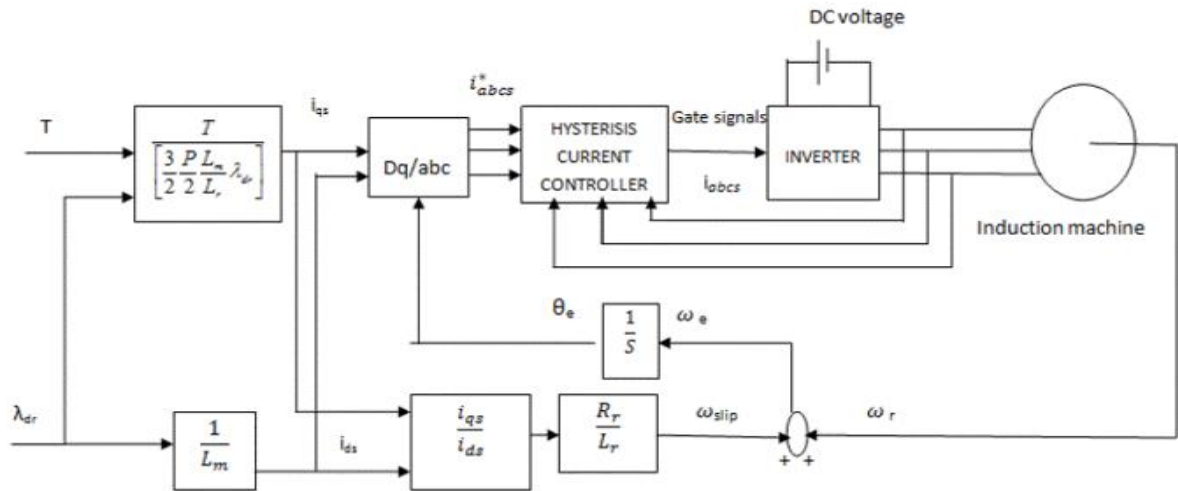


Figure 3.3 Block diagram of indirect rotor field oriented control scheme

3.4 DQ-TO-ABC Transformation

This transformation is called Inverse Clarke's transformation :

$$\begin{bmatrix} I_a^* \\ I_b^* \\ I_c^* \end{bmatrix} = \frac{2}{3} \begin{bmatrix} \cos(\theta) & -\sin(\theta) \\ \cos(\theta - \gamma) & -\sin(\theta - \gamma) \\ \cos(\theta + \gamma) & -\sin(\theta + \gamma) \end{bmatrix} \begin{bmatrix} I_d^* \\ I_q^* \end{bmatrix}, \text{ where } \gamma = 2\pi/3.$$

The induction motor model in the synchronous reference frame is given by:

$$V_{qs} = (R_s + L_s P) i_{qs} + W_s L_s i_{ds} + L_m P i_{qr} + W_s L_m i_{dr} \quad (3.8)$$

$$V_{ds} = -W_s L_s i_{qs} + (R_s + L_s P) i_{ds} - W_s L_m i_{qr} + L_m P i_{dr} \quad (3.9)$$

$$V_{qr} = L_m P i_{qs} + (W_s - W_r) L_m i_{ds} + (R_r + L_r P) i_{qr} + (W_s - W_r) L_r i_{dr} \quad (3.10)$$

$$V_{dr} = -(W_s - W_r)L_m i_{qs} + L_m P i_{ds} + (W_s - W_r)L_r i_{qr} + (R_r + L_r P)i_{dr} \quad (3.11)$$

The stator and rotor flux linkages in electrical synchronous reference frame are given by:

$$\Psi_{qs} = L_s i_{qs} + L_m i_{qr} \quad (3.12)$$

$$\Psi_{ds} = L_s i_{ds} + L_m i_{dr} \quad (3.13)$$

$$\Psi_{qr} = L_r i_{qr} + L_m i_{qs} \quad (3.14)$$

$$\Psi_{dr} = L_r i_{dr} + L_m i_{ds} \quad (3.15)$$

Substituting the corresponding values, the rotor flux is given by:

$$\Psi_{r, rated} = \sqrt{\Psi_{qr}^2 + \Psi_{dr}^2} \quad (3.16)$$

3.5 Field weakening control

Over rated speed operation is obtained by reducing the flux reference inversely proportional to the reference speed (Field weakening region).

The value of the reference flux is calculated according to the following expression:

$$\Psi_r^* = \begin{cases} \Psi_{r, rated}^* & \text{if } W_{r, ref} \leq W_{r, rated} \\ \Psi_{r, rated}^* * \frac{W_{r, rated}}{W_{r, ref}} & \text{if } W_{r, ref} > W_{r, rated} \end{cases} \quad (3.17)$$

3.6 Hysteresis band Pulse Width Modulation current control 'PWM HBPWM'

The HBPWM is basically an instantaneous feedback current control method of PWM where the current continually tracks the command current within a specified hysteresis band.

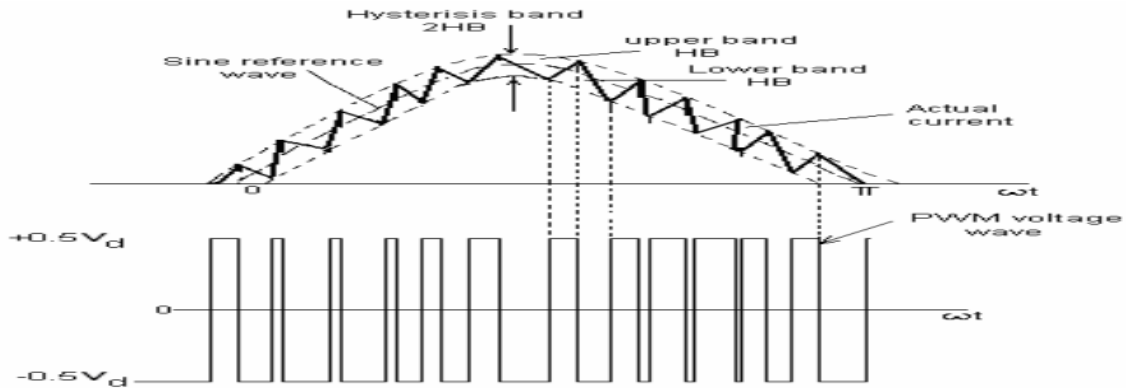


Figure3.4 Principle of hysteresis band current control

The **Figure 3.4** explains the operation principle of HBPWM. The control circuit generates the sine reference current wave of desired magnitude and frequency, and it is compared with the actual phase current wave. As the current exceeds a prescribed hysteresis band, the upper switch is turned off and the lower switch is turned on. As a result, the output voltage transitions from $+0.5V_d$ to $-0.5V_d$, and the current starts to decay. As the current crosses the lower band limit, the lower switch is turned off and the upper switch is turned on. The actual current wave is thus forced to track the sine reference wave within the hysteresis band by back- and-forth switching of the upper and lower switches. The inverter then essentially becomes a current source with peak to peak current ripple, which is controlled within the hysteresis band irrespective of V_d fluctuation. Then the current increases again and the process is constantly repeated to keep the ripple at the desired range. The peak-to peak current ripple and the switching frequency are related to the width of the hysteresis band (as Δi increase the frequency decreases). The inputs to the HBPWM controller are three phase current errors and the outputs are the switching patterns to the PWM inverter [3].

The hysteresis current controller is applied three-phase in a similar way to the single system, but all phases should be under hysteresis control separately. The conditions for switching the devices are noted below:

$$\begin{cases} \text{Upper switch ON or } U = 1 & \text{for } (I^* - I) > HB \\ \text{Lower switch ON or } U = -1 & \text{for } (I^* - I) < -HB \end{cases}$$

Where U is the output of the hysteresis block and HB is the hysteresis bandwidth.

In the hysteresis current controller of **Figure 3.4**, load currents I_a , I_b and I_c are respectively forced to follow reference currents I_{aref} , I_{bref} and I_{cref} within a hysteresis band by the switching action of the inverter. The upper and lower bonds of the hysteresis band are set for the motor current, and the hysteresis controller logic control can be described according to the following rules (the switches notation follows the **Table 2.1**):

Rule A:	For	$I_{aref} > 0 :$	$S_{12}=0,$
	If	$I_a > I_{aref} + \Delta i$	Then $S_{11} = 0,$
	Else If	$I_a < I_{aref} - \Delta i$	Then $S_{11} = 1,$

	Else	no change.	
Rule B:	For	$I_{aref} < 0 :$	$S_{11}=0,$
	If	$I_a > I_{aref} + \Delta i$	Then $S_{12} = 0,$
	Else If	$I_a < I_{aref} - \Delta i$	Then $S_{12} = 1,$
	Else	no change.	

The main drawback of this method is that the PWM frequency is not constant.

3.7 Conclusion

This chapter covered different Rotor field-oriented control components' laws, the DQ-TO-ABC Transformation and the Hysteresis band Pulse Width Modulation current control 'PWM HBPWM' principle of operation as it is the current control for the inverter.

Chapter 04: Simulation results

4.1 Introduction

The Field Oriented Control technique needs more calculations than the other control methods: parameters of the motor, peak values of currents and the value of the slip speed for rated torque operation, selection of the DC voltage etc. It is also necessary to determine the parameters of the speed PI controller-Kp & Ki. This chapter presents the simulation part of an indirect rotor field orientation and starts with calculations for parameter determination of the Induction motor under test, and describes the calculations required for design of Indirect Rotor Field orientation control scheme. the SIMULINK model is developed for Indirect Rotor Field Oriented Induction motor using MATLAB 2016. The motor used for the test is 4 poles 3 phase induction motor with a rated power of 1.5 kw.

4.2 Calculations for parameter determination

The following tests are used to determine motor parameter:

4.2.1 DC test

The purpose of this test is to determine the stator resistance, a variable dc voltage source is adjusted to provide approximately rated stator current and the resistance between the two stator leads is determined from the reading of voltmeter and ammeter [14], then:

$$R_{DC} = \frac{V_{DC}}{I_{DC}} \quad (4.1)$$

If the stator is Y-connected, then the per phase stator resistance is

$$R_s = \frac{R_{DC}}{2} \quad (4.2)$$

If the stator is delta-connected, then the per phase stator resistance is

$$R_s = \frac{3 * R_{DC}}{2} \quad (4.3)$$

After performing the test $R_s = 5.1\Omega$

4.2.2 No load test

In this test the motor is allowed to spin freely so the only load in the motor is the friction and windage losses, so all the converted power is consumed by mechanical losses. The slip is very small [14].

The P_{Rcl} is negligible because I_r is extremely small because 'Rr/s' is very large, so the input power equals:

$$P_{in} = P_{scl} + p_{core} + p_{fw} \quad (4.4)$$

The equivalent input impedance is thus approximately

$$|Z|_{eq} = \frac{V_{\phi}}{I_{nl}} \approx X_s + X_m \quad (4.5)$$

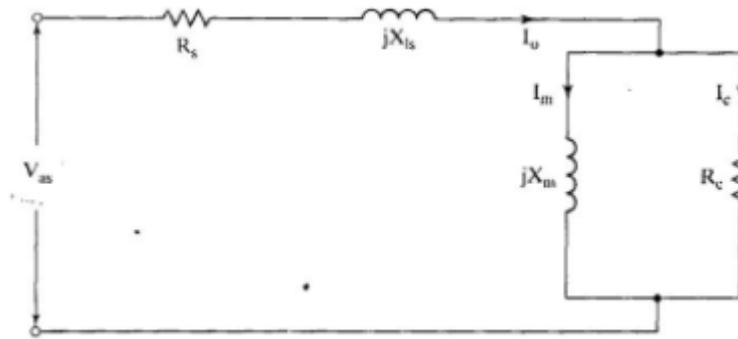


Figure4.1 Equivalent circuit of no-load test

After performing the test: $|Z_{eq}| = \frac{400/\sqrt{3}}{2.1} = X_s + X_m = 109.97 \Omega$

4.2.3 Blocked rotor test

In this test, the rotor is locked or blocked so that it cannot move, so $S=1$ a voltage is applied to the motor, and the resulting voltage, current and power are measured.

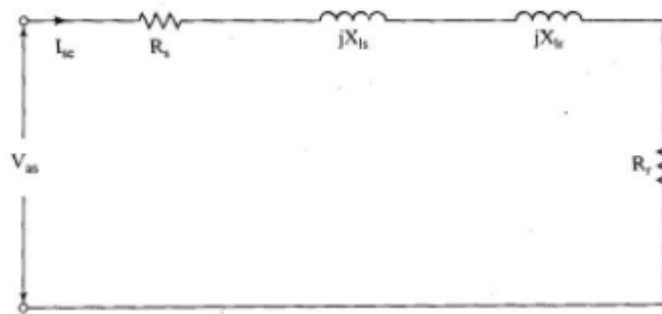


Figure4.2 Equivalent circuit of blocked rotor test

The AC voltage applied to the stator is adjusted so that the current flow is approximately full-load value. The locked-rotor power factor can be found as

$$PF = \cos\theta = \frac{P_{in}}{\sqrt{3}V_l I_l} \quad (4.6)$$

The magnitude of the total impedance is

$$|Z|_{LR} = \frac{V_\phi}{I_{LR}} \quad (4.7)$$

$$|Z_{LR}| = R_{LR} + jX_{LR} = |Z_{LR}| \cos\theta + j|Z_{LR}| \sin\theta \quad (4.8)$$

$$R_{LR} = R_s + R_r \quad (4.9)$$

$$X_{LR} = X_s + X_r \quad (4.10)$$

After performing the test, the following values are measured:

$P_{in}=245\text{w}$, $V\text{-line}=86\text{v}$, $I\text{-line}=3.5\text{A}$.

$X_{LR} = X_s + X_r = 12.49 \Omega$ and $R_{LR} = R_s + R_r = 6.66 \Omega$ So $R_r = 1.566\Omega$

The connection between X_1, X_2 for the most common types of industrial Induction motors is grouped by the National Electrical Manufacturer's Association (NEMA) and according to the type of the motor used in the tests (B type design) $X_s = 0.4X_{LR}$ and $X_r = 0.6X_{LR}$ so $L_s=0.0159 H$ and $L_r=0.02388 H$ and from the no load test we deduce that $L_m=0.334 H$

4.2.4 Mechanical parameters determination

The determination of the viscous friction coefficient and the moment of inertia is based on the measurement of mechanical losses when the machine is running at a given speed and also on the reading of the slowdown curve. The following equation is used to find the inertia:

$$J = \frac{P_m}{\omega_r * \left(\frac{d\omega}{dt}\right)} \quad (4.16)$$

Where ω_r is the rated mechanical speed (rad/s) and $\frac{d\omega}{dt} = \frac{\Delta\omega}{\Delta t}$ where Δt and $\Delta\omega$ are obtained from slowdown curve as following

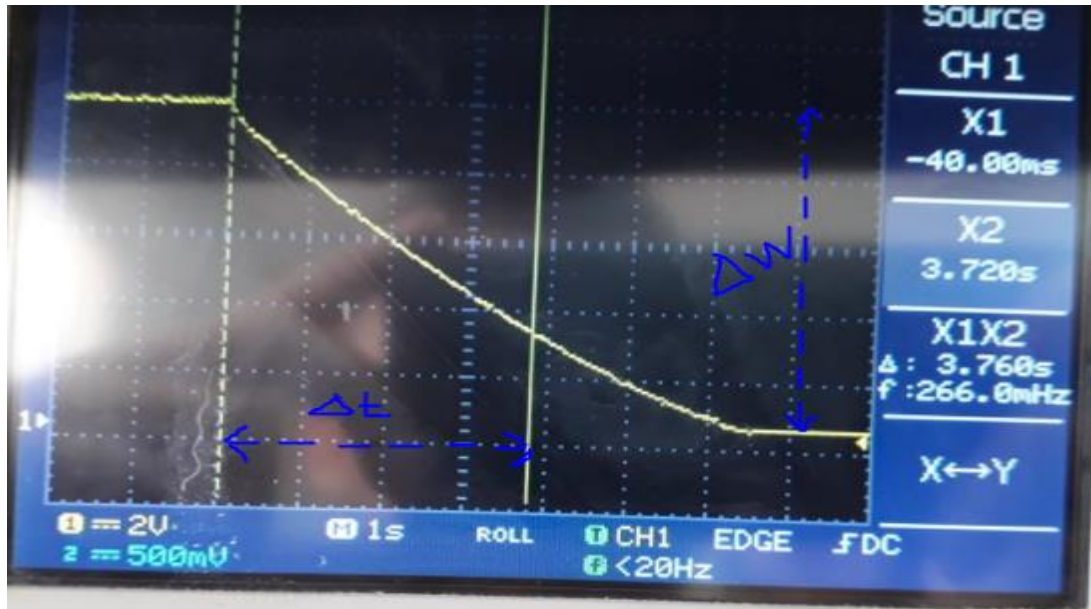


Figure4.3 Slow down curve

From the cursor measurements $\Delta t = 3.76 \text{ s}$ and $\Delta \omega = \omega_r = 1408 \text{ rpm}$.

Now we look for the mechanical power losses, we measure the power/voltage/current at different values of voltage in the no load test then we calculate power losses, the obtained results are illustrated in the next table:

Table 4.1 Active and reactive power computations at different voltages

$V = \sqrt{3}V_s$	I(A)	P(watts)	Q(VAR)	P_{scl}	$P_{CL} + P_m$	$3V_s^2$
400	2.1	260	1489.56	67.473	192.527	160000
360	1.65	170	987.26	41.654	128.346	129600
320	1.34	130	710.14	27.473	102.527	102400
280	1.10	90	536.94	18.513	71.487	78400
240	0.97	70	363.73	14.396	55.604	57600
200	0.76	50	259.81	8.837	41.163	40000
160	0.58	45	199.18	5.147	39.853	25600

Now using MATLAB, we plot graph of $P_{CL} + P_m$ versus $3V_s^2$ it should be a direct line [15]. But due to errors in measurement it is not so we draw a line from rated value that best

fits the values When $3V_s^2$ equals zero the only losses remaining in the motor are the mechanical losses [15]. Which corresponds to $P_m = 80 \text{ w}$.Now Using the previous equation

$$j = 0.013 \text{Kgm}^2$$

At no load test we only have the friction torque as a load so we can find the friction factor

Using the following equation

$$T_L = f * \omega_m \quad (4.17)$$

At speed of 1408 rpm we measure a torque of 0.45Nm so $f = 0.00305 \text{ Nm}/(\text{rad}/\text{s})$.

4.3 Proposed methodology and its design

4.3.1 Calculation of rated torque

Under no-load & rated condition, rated torque is given by

$$T_L = \frac{P_n}{\omega_n} = \frac{1500}{1410 * \frac{2\pi}{60}} = 10.1 \text{ Nm} \quad (4.18)$$

4.3.2 Calculation of rated flux

Using the results of current /voltage/power obtained from the no load test and taking in consideration that $I_r = 0$,the rated flux is calculated according to equations (3.14), (3.15), (3.16).

$$\Psi_{r-rated} = 1.1 \text{ Wb}.$$

4.3.3 Speed controller

The most commonly used controller for the speed control of induction motors is conventional PI controller. The transfer function of PI controller is given by:

$$G(S)_c = \frac{K_p S + K_i}{S} \quad (4.19)$$

Proportional gain and the integral gain, K_p & K_i , are the parameters of PI controller. These parameters are determined using manual tuning technique. In manual tuning process, initially K_p was kept equal to 1 & K_i equal to 0.0001. Then, K_p was increased till the output shows some oscillations. Then K_i was changed to remove steady state error [16].

4.3.4 Selection of dc voltage

The induction motor is fed by a current-controlled PWM inverter the fundamental rms line-to-line voltage is [17]:

$$V_{L-L} = 0.45 * \sqrt{3} * V_{DC} \quad (4.20)$$

$$V_{DC} \gg \frac{V_{L-L}}{0.612} \quad (4.21)$$

So the inverter is built with Vdc= 513Volts.

4.4 Development of simulink model

Based on the equations presented in chapter 3 and using various tool boxes available in the SIMULINK library, model is developed for each block. Step by step development of model is presented here.

4.4.1 Speed regulator block

The simulink model of it is implemented as shown in the next Figure:

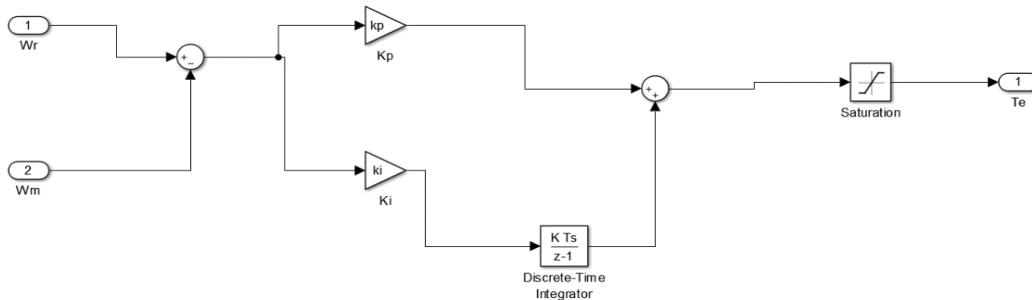


Figure4.4 Speed regulator block

4.4.2 IRFOC block

This block is implemented as shown in **Figure4.5** It consists of 5 main sub-blocks I_{ds}^* computation, I_{qs}^* computation, dq-to-ABC transformation, Slip computation and theta computation blocks. The Simulink models are built Based on previous equations of chapter 3.

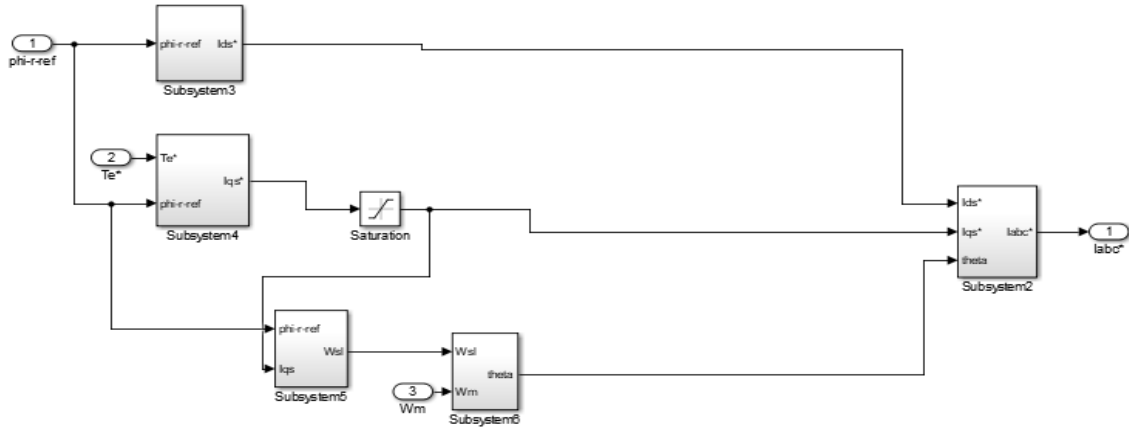


Figure4.5 IRFOC block

4.4.3 Current regulation

Current regulator used in this field-oriented control is hysteresis band current controller. It is one of the several types of PWM techniques. It is basically a feedback current control method of PWM where the actual currents are compared with the reference currents within the specified hysteresis band. Thus, the inputs to the Hysteresis controller are three phase current errors and the outputs are the switching pulses to the inverter. **Figure.4.6** bellow shows the Simulink model of Hysteresis current controller:

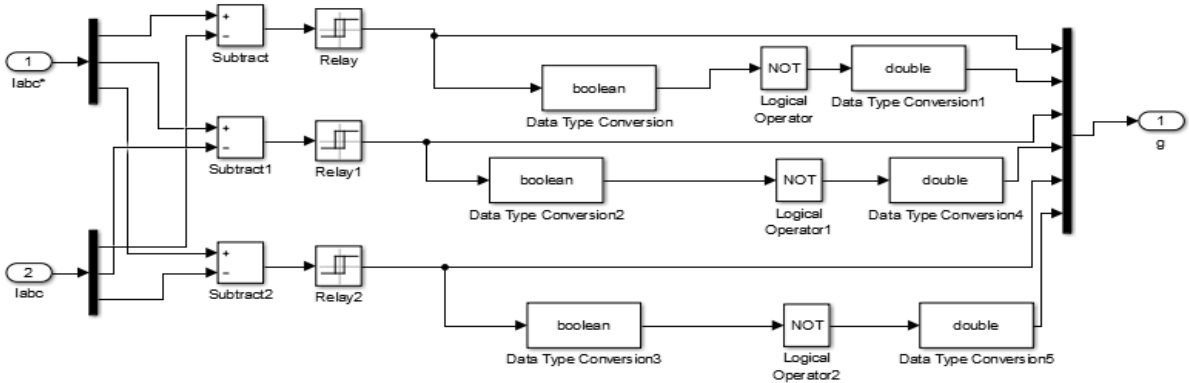


Figure4.6 Simulink model of hysteresis current controller

4.4.4 Simulink model of Indirect Rotor Field Oriented Induction Motor

Now we connect all subblocks as following:

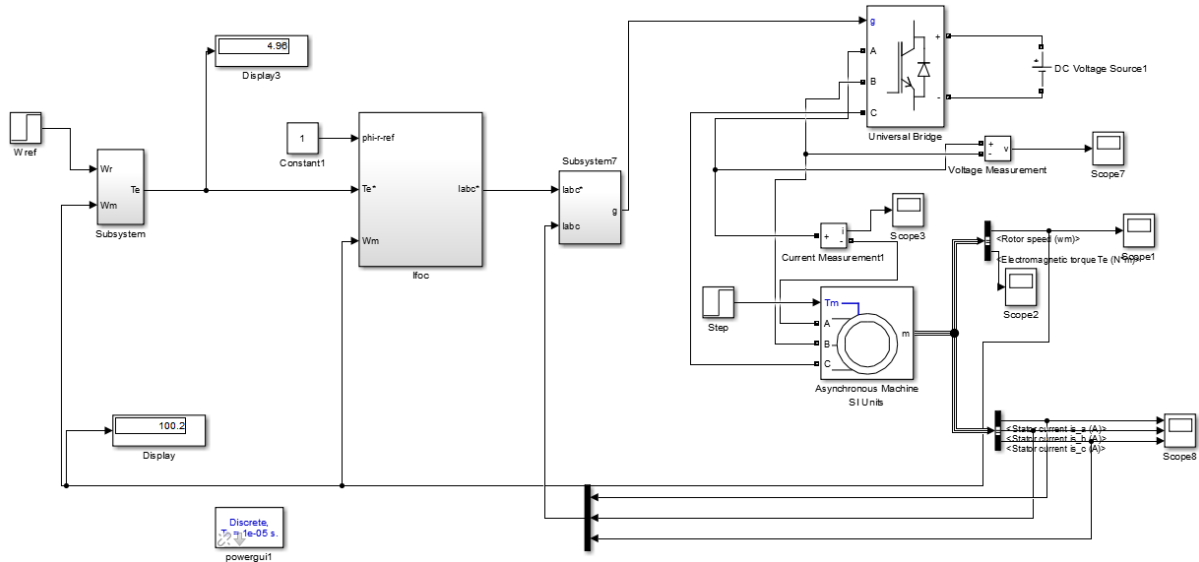


Figure4.7 Model of indirect rotor field oriented induction motor

4.5 Setting of the simulation parameters

Initially the reference speed is set to a constant value of 100 rad/s (955rpm) and the load torque is also kept constant at 0 N-m. Setting the correct parameters of the speed PI controller and hysteresis band is an important task in simulating the model for getting the accurate results. The values of K_p , K_i and hysteresis band h are to be adjusted number of times and simulation is run every time until accurate results are obtained. There are many frequency domain and time domain methods available for designing of a PI controller. But all these methods do not guarantee that the controller parameters found by them gives you accurate performance characteristics. They just give the initial guess for the controller parameters and finally you have to tune the controller manually.

Here the speed PI controller is tuned manually. The simulation is run for the 3 sec and the responses are observed on the respective scopes. After performing many tests, the values are set as following $K_i = 0.15$, $K_p = 8.5$, $h = 0.05$.

Now to verify the stability of our system we should find the transfer function relating the torque to speed as illustrated in the following figure

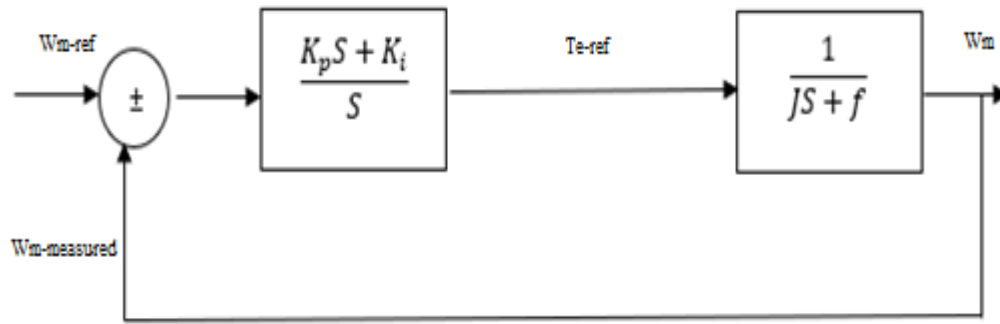


Figure4.8 Transfer function relating the torque to speed

Where the input is the mechanical reference speed compared with the feedback measured speed.

The first block represents the speed regulator block the input of this block is the speed error and its output is the reference torque. The second block represents the torque equation for rotating system obtained from the following relation:

$$T_e(t) = J * \frac{dw_m(t)}{dt} + f * w_m \quad (4.22)$$

Where J is inertia of equivalent motor-load system (kgm^2) and f represents the friction.

Rewriting it using Laplace transform

$$\frac{w_m(s)}{T_e(s)} = \frac{1}{Js+f} \quad (4.23)$$

The total transfer function of the system is given as follows:

$$G_t = \frac{K_p S + K_i}{S^2 + \frac{S(f+K_p)}{J} + \frac{K_i}{J}} \quad (4.24)$$

Replacing all the values in the transfer function and solving the denominator equation leads to negative poles which means that our system is stable [18].

4.6 Simulation results and discussion

Part1

In this part the speed is set to 100 rad/s and the load torque to 4 Nm the observed speed, output torque, output rotor flux components and currents are shown in the next figures

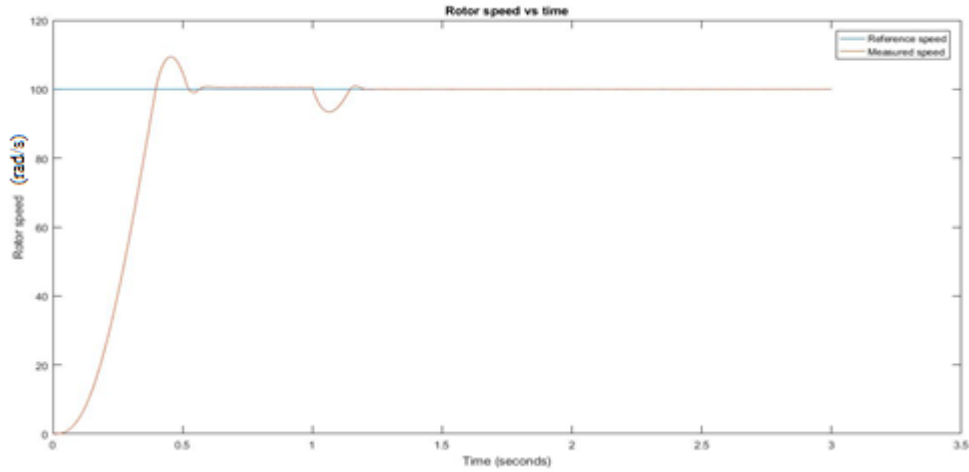


Figure4.9 Rotor speed vs time

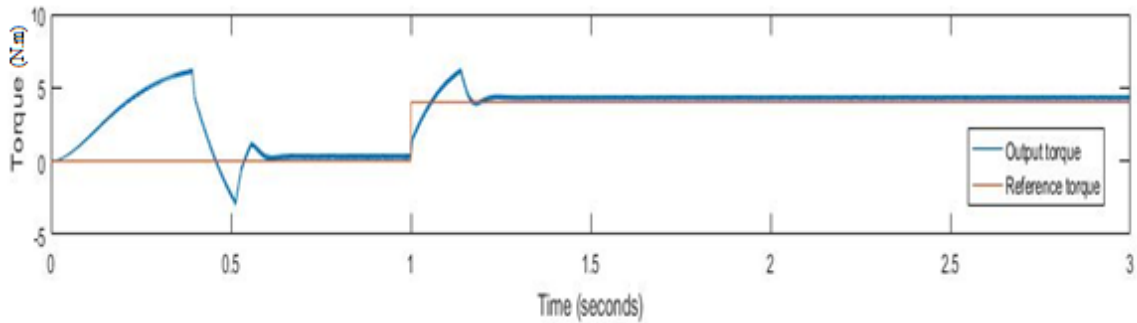


Figure4.10 Output torque

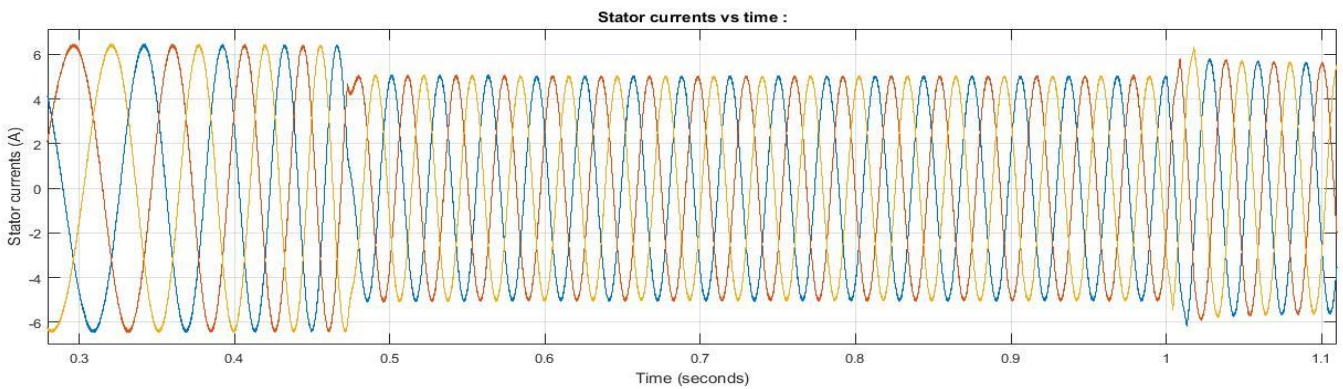


Figure4.11 Stator currents

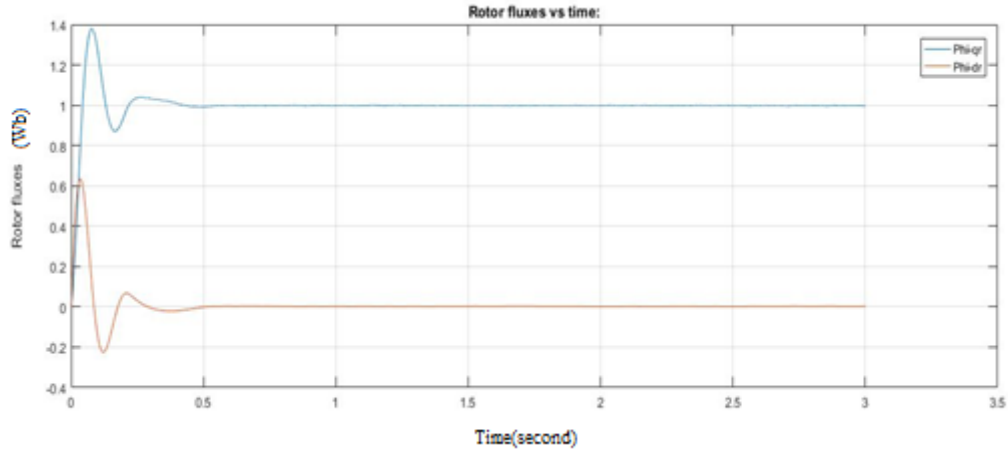


Figure4.12 Rotor fluxes

Part2

In this part the speed is set to 80 rad/s then at $t = 2s$ the speed is changed to 100 rad/s the following figures shows the speed variation, w_{sl} variation and the frequency variation of the currents:

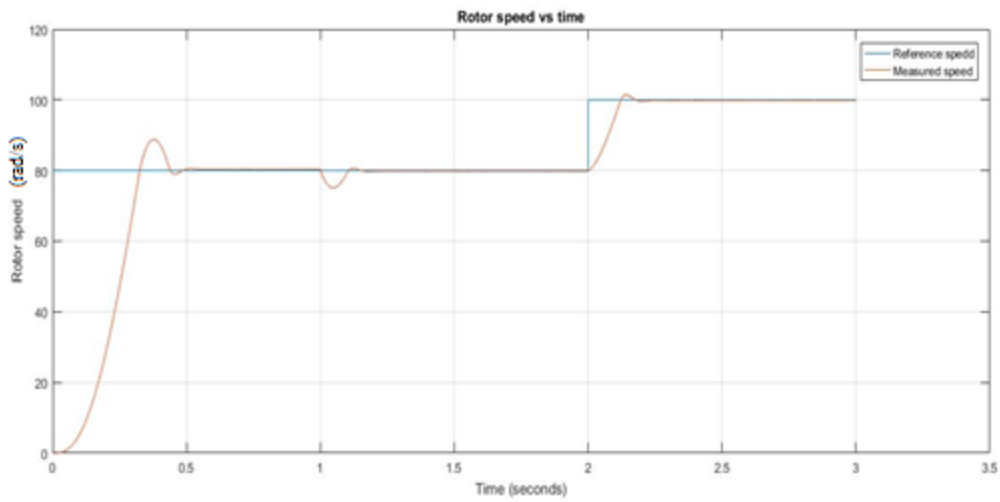


Figure4.13 Rotor speed

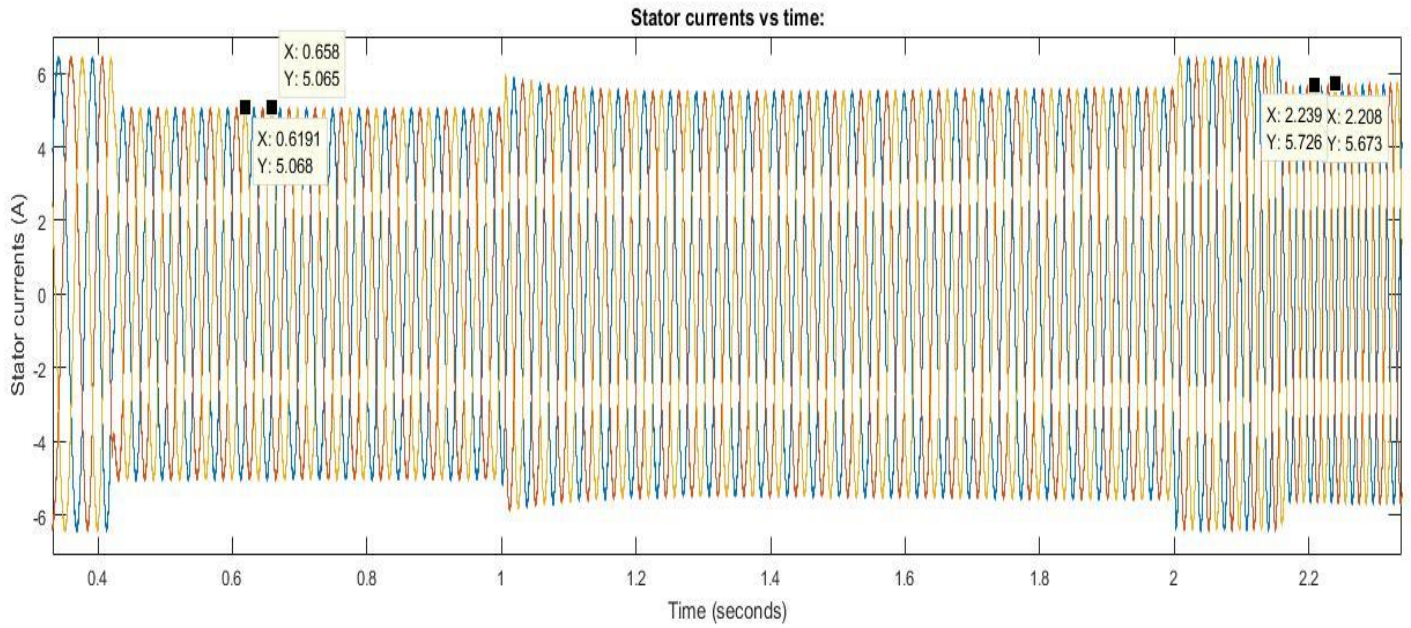


Figure 4.14 Stator currents

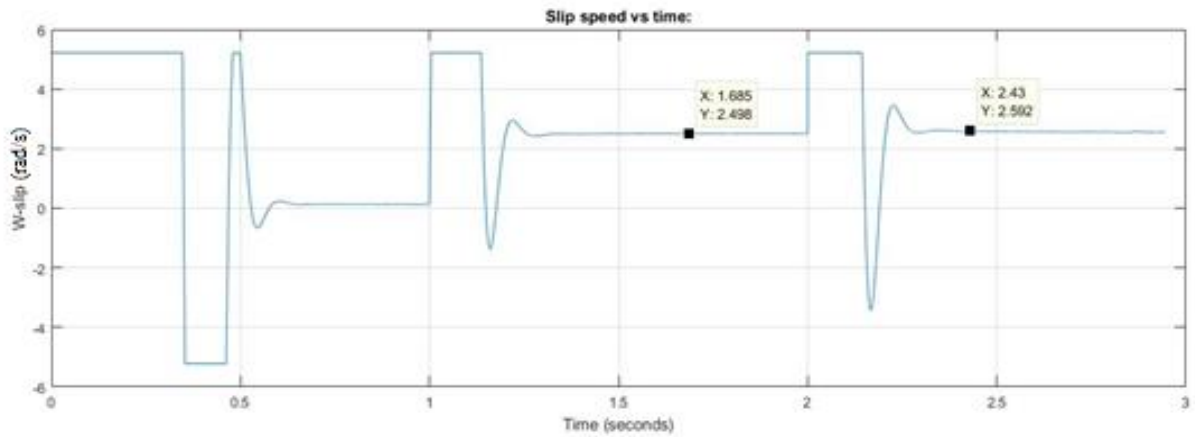


Figure 4.15 Slip speed

Discussion

The frequency of one phase of current is calculated from the data of **Figure 4.14** before 2s which corresponds to the applied reference speed of 80 rad/s and then after 2 s which corresponds to the applied reference speed of 100rad/s.

$f_1 = 25.64 \text{ Hz}$, $f_2 = 32.25 \text{ Hz}$ From those frequencies the applied synchronous speed is calculated: $W_{sy-1} = 80.55 \text{ rad/s}$, $W_{sy-2} = 101.31 \text{ rad/s}$.

The electrical slip speed W_{sl} that corresponds to the mentioned frequencies is showed in **Figure 4.15**: $W_{sl-1} = 2.498 \text{ rad/s}$, $W_{sl-2} = 2.592 \text{ rad/s}$.

Now the rotor speed W_r is calculated according to the previous data:

$W_{r-1} = 79.33 \text{ rad/s}$ which corresponds to the reference speed of 80 rad/s.

$W_{r-2} = 100.04 \text{ rad/s}$ which corresponds to the reference speed of 100 rad/s.

4.7 Conclusion

In this chapter detail calculations necessary for the development of the Indirect rotor field-oriented control of induction motor drive using Matlab/ Simulink has been presented. The model so developed can be used to study the dynamic behavior of the induction motor by applying step change in the reference speed and the load torque.

Chapter 05:
Implementation and
discussion

5.1 Introduction

This chapter deals with the experimental setup of the implementation of the VFD control, based on the background introduced in the previous chapters and the simulation done in chapter 04 to consolidate the theoretical analysis of this thesis.

The experimental work was conducted in the Power Research Laboratory at the Institute of Electrical and Electronic Engineering of Boumerdes University. The implementation is conducted for an asynchronous three-phase squirrel cage 1.5kW induction motor using a DSP tms320f28027f.

Many control systems utilize powerful high-performance microcontrollers in order to meet real-time design requirements. In addition to the microcontroller, these systems require various analog components to sense signals for the feedback control loops, as well as for hardware protection. Some advanced control systems may even require two microcontrollers: for example, one can be used to track speed and position, while the other can be used to control torque and current loops. Ideally, combining the two microcontrollers with a common communication link between them, along with the necessary analog components into a single device would increase system performance and reliability, and at the same time simplify the board layout and reduce the overall system cost. [19]

5.2 Operation description

To assess the control strategy presented in this thesis in real time, an experimental test bench shown in **Figure5.3** is built. The present work consists of a DC power supply supplying an inverter feeding a 1.5 kW 4 poles squirrel cage induction motor. The control algorithm is implemented via a DSP TMS320f28027f Piccolo from Texas Instruments. The utilized inverter and the different sensors needed for IRFOC are designed by **EURL MICROTECH SYSTEMS DESIGN**. Those sensors ensure the measurement of current using ACS710 sensor. These current circuits are used essentially to measure the actual current for both phases a and b under any operating condition. Whereas the rotor speed is measured using the Taco generator.

5.3 DSP Description

C2000™ 32-bit (CPU) microcontrollers are optimized for processing, sensing, and actuation to improve closed loop performance in real-time control applications such as industrial motor drives; solar inverters and digital power; electrical vehicles and transportation; motor control; and sensing and signal processing. The C2000 line includes the Delfino™ Premium Performance family and the Piccolo™ Entry Performance family [20].

The F2802x Piccolo™ family of microcontrollers provides the power of the C28x core coupled with highly integrated control peripherals in low pin-count devices.

This family is code-compatible with previous C28x-based code, and also provides a high level of analog integration and the ADC converts from 0 to 3.3-V.

5.4 Current sensor circuit

The ACS 710 hall effect transducer was used in order to sense the current. The ACS710 consists of a precision linear Hall sensor integrated circuit with a copper conduction path. Applied current flows through the copper conduction path, and the analog output voltage from the Hall sensor linearly tracks the magnetic field generated by the applied current for the case of the motor currents, we have an AC signal thus an offset is introduced in order to shift the current signal and map it in the positive quarter [21]. Its circuit is implemented within the module containing the inverter and sensors, with a linear ratio of:

$$V_{out} = I_{in} * 56mV \quad (5.1)$$

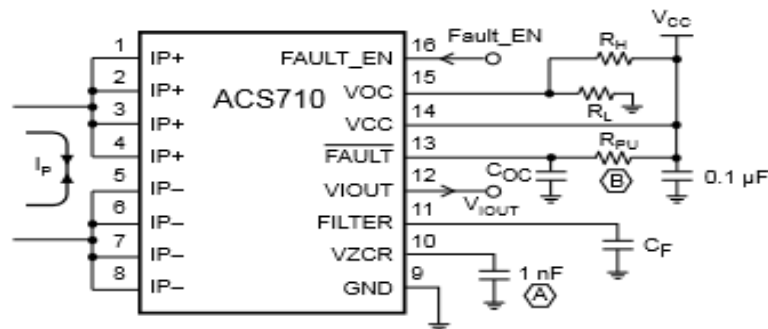


Figure5.1 Current sensor circuit.

5.5 Speed Measurement Circuit

The output of the Taco generator is 92.4V for the rated Speed of 1410 rpm. To convert this information a divider circuit was implemented to regulate the voltage in the range of 0 to 3.3 v with gain of:

$$V_{out} = \frac{3.3}{92.4} * V_{in} \quad (5.2)$$

The following Figure shows all of the module components (DSP, inverter, current sensor and the divider circuit):

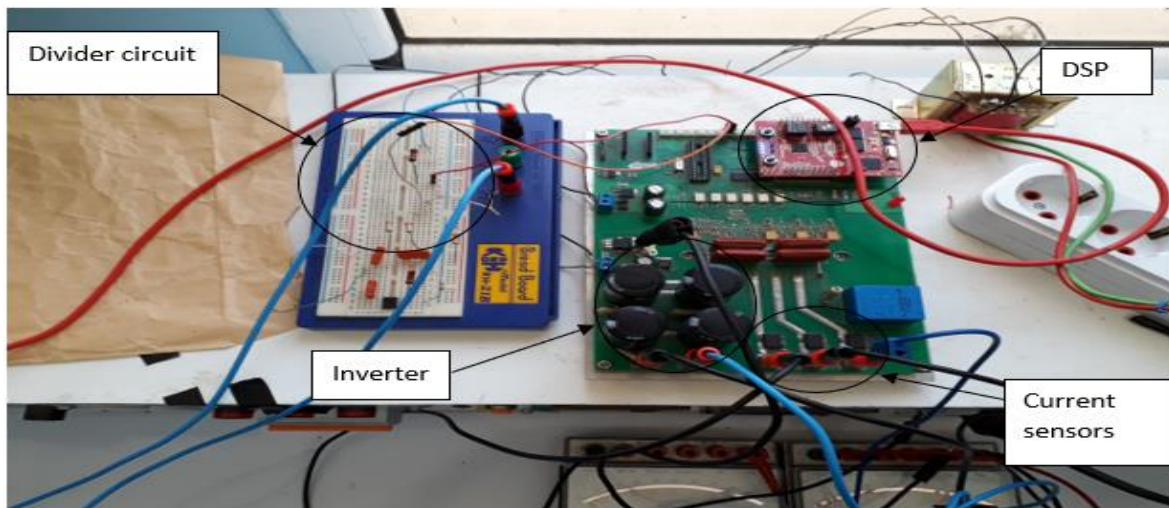


Figure5.2 All of the module components

5.6 Software implementation

The VFD algorithm was implemented using 12bit DSP TMS320F28027f card. In order to program this card, we have used MATLAB/Simulink C2000 tools.

5.6.1 The ADC assignment

In this implementation, three ADCs have been used which are ADCINA0, ADCINA1, ADCINA3 and. These ADCs were used in order to measure:

- Induction motor Currents (phase a, and phase b).
- The speed from the tachometer.

The used DSP ADCs can accept a voltage between [0-3.3] V, therefore a software compensation must be added in order to remove the incorrectness of the read value. Thus, a calibration of the ADC is a must.

5.6.2 Calibration of the ADC of DSP TMS320f28027f

For the current sensor the Analog to digital conversion is expressed as follow:

$$D = \text{input voltage} * 4096 / 3.3 \quad (5.3)$$

D is the Digital output of the ADC ranging from 0 to 4096(2^{12}).

Now to recover the real measured signal from the digital value, the used expression is:

$$X = D * 3300 / (4096 * 56) \quad (5.4)$$

Where X is the recovered current signal.

Then for the Taco generator the gain applied after the ADC is:

$$W_r = \frac{148}{4096} \text{ (rad/s)} \quad (5.5)$$

5.6.3 G.P.I.O configuration

The GPIO shows the state of the IRFOC algorithm. The used GPIO pins were configured according to the pins' location with respect to the module design (see Appendix A). The GPIO represents the switching control signals generated in order to control the switch ON/OFF of the inverter.

5.7 Hardware implementation

The following Figure shows all the components previously discussed combined into the real implementation of IRFOC:



Figure5.3 Implementation test bench

5.8 Implementation results

The implementation was conducted in two sets of operation, openloop and closed loop operation.

5.8.1 Open loop operation

The following Figure represents the openloop operation algorithm:

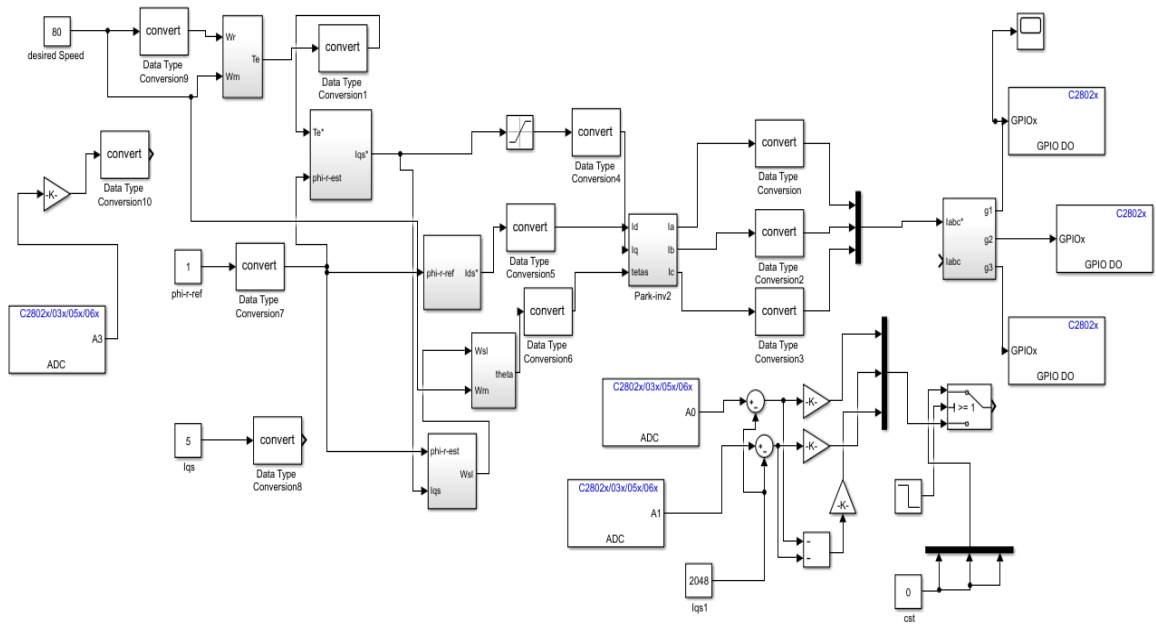


Figure5.4 Openloop operation algorithm

The reference speed is set to 80 rad/s, the resulting current waveform was measured through two current probes and the gate signals were both displayed in the oscilloscope Gwinstek GDS-1042:



Figure5.5 Current Probes

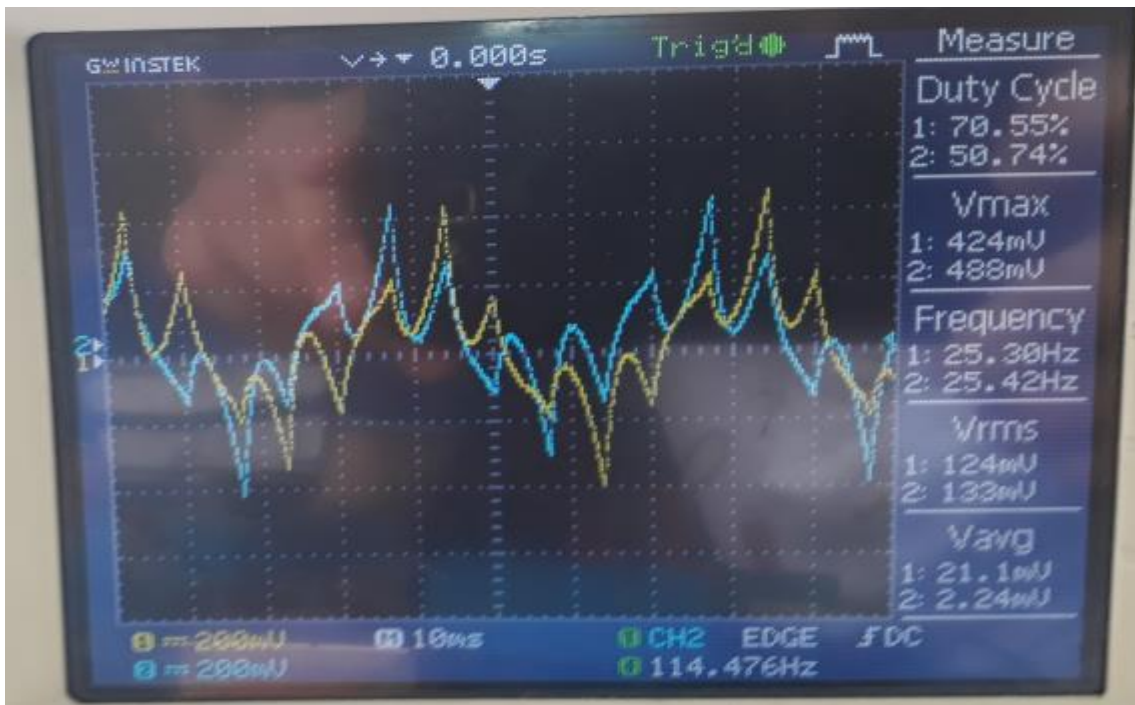


Figure5.6 Current Waveforms

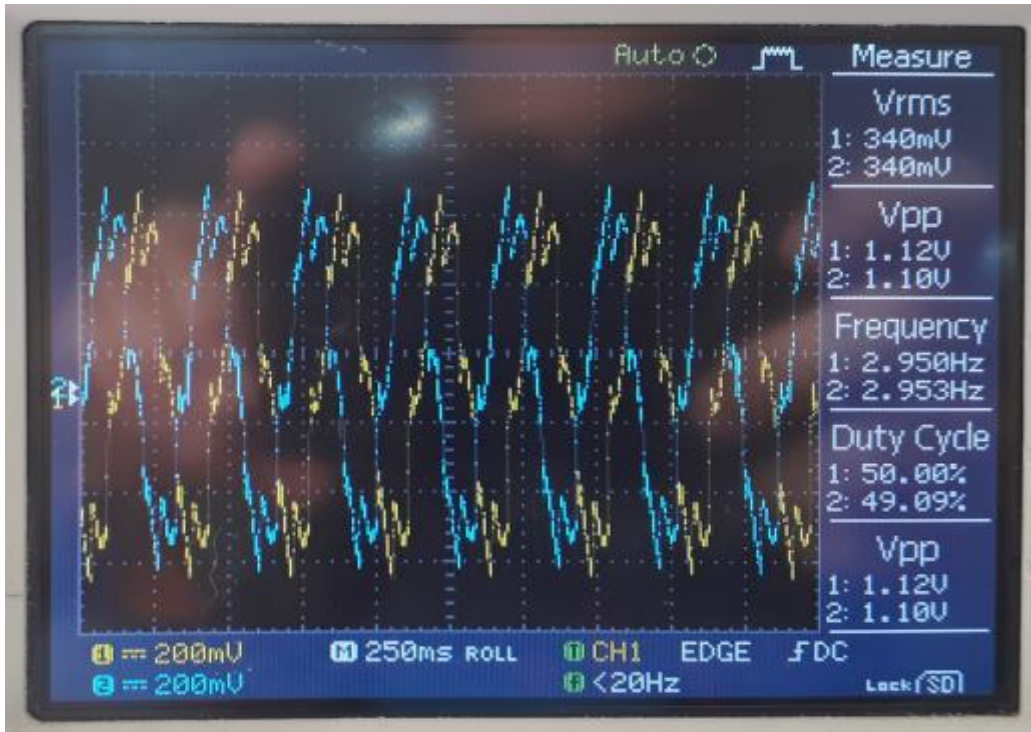


Figure5.9 Current waveform

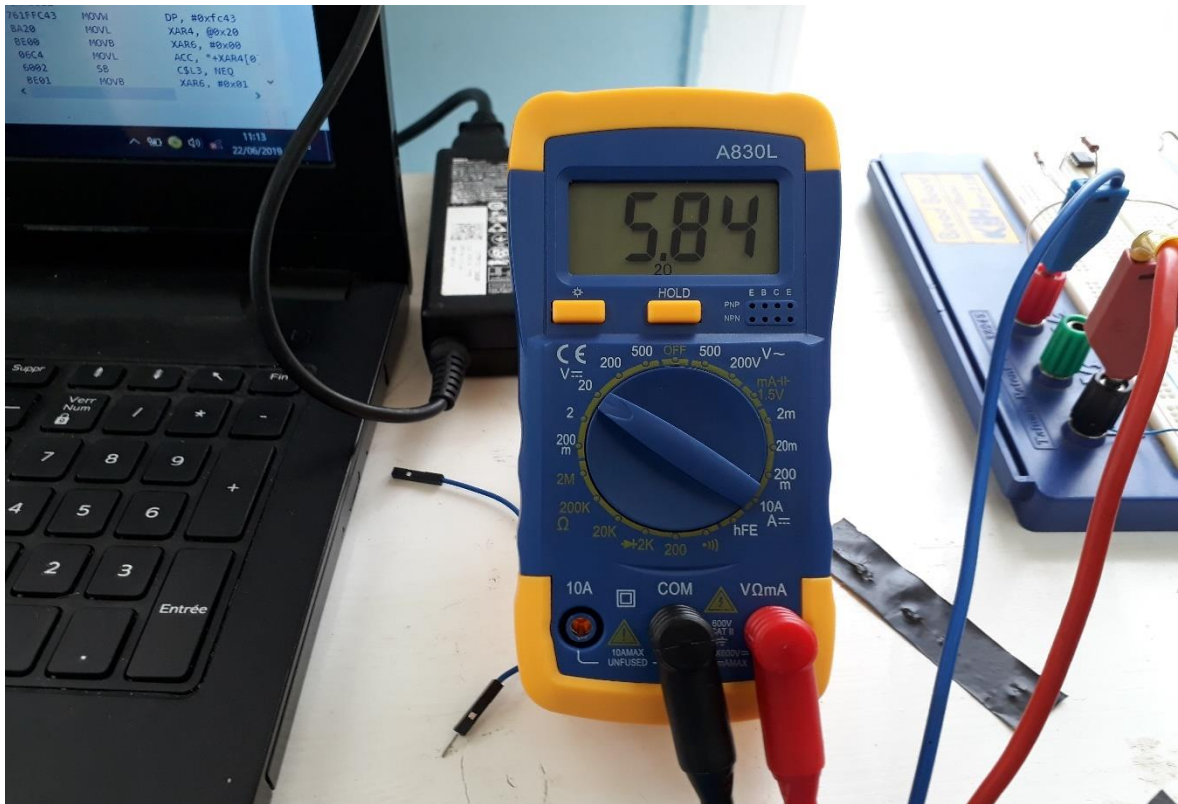


Figure5.10 Speed measurement of taco generator

Discussion

The resulting current waveform are closer to a sinusoidal waveform which means they are of higher precision and accuracy than the openloop currents ,but still are not ideal , that is due to a drift in the the measurements of current sensors and small deficiency in the different equipments.The frequency of the measured current (2.95Hz) corresponds to the reference speed of 10 rad/s and also to the taco generator measured voltage.

5.9 Conclusion

This chapter covered the implementation setup and results of the conventional IRFOC control drive for an induction motor.

It has been noticed that the implementation and simulation results are approximately the same but with small difference due to some limitations and constraints in the hardware implementation, such as:

- Sensor offset.
- Motor losses as the d-q model and its inverse are not an exact model for the motor as it doesn't take into consideration the different losses.

From this implementation it can be concluded that this technique is a suitable control technique.

General conclusion

This master thesis validates the proposed model of the variable frequency drive (specifically indirect rotor field-oriented control) of 3 phase induction motor as an efficiently working vector control technique. This technique was preferred over the others due to its simplicity, high performance and fast dynamic in motor control. Also, the chosen PWM technique proved its efficiency as observed in the simulation results.

The designed code was implemented using Matlab/Simulink C2000 package for the C2802x. This programming way is simple and cheap since the size and cost of the system are decreased and the efficiency is high in concordance with the theoretical results that were to be expected. In the implementation, both the open and closed loop operations of three phase induction motor using indirect rotor field-oriented control have been implemented, showing that the TMS320F28027F board was effective and capable of controlling our system.

Along this dissertation, it has been noticed that the experimental results matched the simulated ones which means that the proposed algorithm was suitable and effective. Also, it is a low cost strategy drive which requires a low number of ADCs, in order to measure the phase currents and speed.

References

- [1] <http://electricalarticle.com/advantages-disadvantages-induction-motor,21/03/2019> .
- [2] <https://www.quora.com/What-is-the-difference-between-FPGA-and-DSP-boards,21/03/2019> .
- [3] <http://chettinadtech.ac.in/storage/12-07-12/12-07-12-10-43-28-1527-Thenmozhi.pdf> ,25/03/2019.
- [4] Pr.Khaldoun A. EE533 Eletrical Drives, chapter5, p27,28, IGEE, Boumerdes, 2019.
- [5] <https://www.electricalclassroom.com/soft-starters-v-s-vfds-variable-frequency-drives-difference-between-soft-starters-and-vfds-selection-soft-starters-v-s-vfds/,28/03/2019>.
- [6] Pr.Khaldoun A. EE533 Eletrical Drives, chapter6, p2, IGEE, Boumerdes, 2019.
- [7] <https://pdfs.semanticscholar.org/e01a/0eb2678a3bdc9c4a8fe5cb28015f66c8e4bf.pdf>, 15/04/2019.
- [8] Holtz, J. "The Representation of AC Machine Dynamics by Complex Signal Flow Graphs", in IEEE Trans. Ind. Appl., Vol. 42, No. 3, pp. 263-271.
- [9] Pr.Khaldoun A. EE533 Eletrical Drives, chapter7, p11, IGEE, Boumerdes, 2019.
- [10] J. M. R. Mallaet. al ,Jagan Mohana Rao Mallaand Manti Mariya Das,' A Review on Direct Torque Control of Induction Motor ' ,International Journal of New Technologies in Science and Engineering Vol. 1, Issue. 1,Jan.2014.
- [11] Badder. U and Depenbrock. M ; "Direct self control (DSC) of inverter fed induction machines: A basic for speed control without speed measurement", IEEE Transactions on Industrial Application, Vol. 28, No. 3, pp. 581-588, West German.
- [12] <http://what-when-how.com/motors-and-drives/inverter-switching-devices-motors-and-drives/,22/04/2019>.
- [13] Pr.Khaldoun A. EE533 Eletrical Drives, chapter8, p15, IGEE, Boumerdes, 2019.
- [14] <https://www.javatpoint.com/no-load-and-blocked-rotor-test>, .
- [15] Par Fateh MEHAZZEM, Contribution à 'la Commande d'un Moteur Asynchrone destiné à la Traction électrique' Présentée et soutenue publiquement le 06/12/2010.
- [16] Vivek V. Puranik1, Vijay N. Gohokar2, 'Simulation of an Indirect Rotor Flux Oriented Induction Motor Drive Using Matlab/Simulink', International Journal of Power Electronics and Drive System (IJPEDS) pp. 1693~1704 ISSN: 2088-8694, DOI: 10.11591/ijpeds.v8i4.pp1693-1704, Vol. 8, No. 4, December 2017.

- [17] Pr.Khaldoun A. EE533 Eletrical Drives, chapter7,p4, IGEE, Boumerdes, 2019.
- [18] Dr.Guernan EE352, lecture5 ,p3, IGEE, Boumerdes, 2019.
- [19] The TMS320F2837xD Architecture: Achieving a New Level of High-Performance
Kenneth W. Schachter, C2000Technical Staff pdf
- [20] TEXAS INSTRUMENTS, SPRS523M –november 2008–revised january 2019
TMS320F2802x Piccolo™ Microcontrollers.
- [21] ALLEGRO microsystems ACS710, 120 kHz Bandwidth, High-Voltage Isolation
Current Sensor with Integrated Overcurrent Detection.

Appendix A: Pins of the DSPTMS320F28027F

Mux Value						Mux Value			
3	2	1	0	J1 Pin	J5 Pin	0	1	2	3
			+3.3V	1	1	+5V			
			ADCINA6	2	2	GND			
TZ2	SDAA	SCIRXDA	GPIO28	3	3	ADCINA7			
TZ3	SCLA	SCITXDA	GPIO29	4	4	ADCINA3			
Rsvd	Rsvd	COMP2OUT	GPIO34	5	5	ADCINA1			
			ADCINA4	6	6	ADCINA0			
	SCITXDA	SPICK	GPIO18	7	7	ADCINB1			
			ADCINA2	8	8	ADCINB3			
			ADCINB2	9	9	ADCINB7			
			ADCINB4	10	10	NC			
3	2	1	0	J6 Pin	J2 Pin	0	1	2	3
Rsvd	Rsvd	EPWM1A	GPIO0	1	1	GND			
COMP1OUT	Rsvd	EPWM1B	GPIO1	2	2	GPIO19	SPISTEA	SCIRXDA	ECAP1
Rsvd	Rsvd	EPWM2A	GPIO2	3	3	GPIO12	TZ1	SCITXDA	Rsvd
COMP2OUT	Rsvd	EPWM2B	GPIO3	4	4	NC			
Rsvd	Rsvd	EPWM3A	GPIO4	5	5	RESET#			
ECAP1	Rsvd	EPWM3B	GPIO5	6	6	GPIO16/32	SPISIM0A/ SDAA	Rsvd/ EPWMSYNCI	TZ2/ ADCSOCA
TZ2/ ADCSOCA	Rsvd/ EPWMSYNCI	SPISIM0A/ SDAA	GPIO16/32	7	7	GPIO17/33	SPISOMIA/ SCLA	Rsvd/ EPWMSYNCO	TZ3/ ADCSOCB
TZ3/ ADCSOCB	Rsvd/ EPWMSYNCO	SPISOMIA/ SCLA	GPIO17/33	8	8	GPIO6	EPWM4A	EPWMSYNCI	EPWMSYNCO
			NC	9	9	GPIO7	EPWM4B	SCIRXDA	Rsvd
			NC	10	10	ADCINB6			